Quantitative evaluation and intercomparison of morning and afternoon Moderate Resolution Imaging Spectroradiometer (MODIS) aerosol measurements from Terra and Aqua

Charles Ichoku,[1,2] Lorraine A. Remer,[3] and Thomas F. Eck[4,5]

Received 4 May 2004; revised 1 July 2004; accepted 13 July 2004; published 10 February 2005.

[1] The quality of the aerosol optical thickness (AOT) data retrieved operationally from the Moderate Resolution Imaging Spectroradiometer (MODIS) sensors aboard the Terra and Aqua satellites, over land, and over ocean from 2000 to 2003 (Aqua only from June 2002) were evaluated thoroughly. Terra-MODIS versions 3 and 4 data (T003 and T004) and Aqua-MODIS version 3 data (A003) were independently and comparatively evaluated with collocated AOT from ground-based Aerosol Robotic Network (AERONET) Sun photometers. At 550 nm wavelength, 67.3%, 55.0%, and 55.5% of AOT from T003, T004, and A003, respectively, meet the prespecified accuracy conditions of ±(0.05 + 0.2aot) over land, while about 63.3%, 59.4%, and 62.2% fall within the more stringent range of ±(0.03 + 0.05aot) over ocean. However, when based on equal standards of comparison and regression analysis, aerosol retrievals are much more accurate over ocean than over land. Analysis of MODIS full regional AOT averages from 12 land and 6 oceanic regions shows that aerosol loading exhibits an annual cycle in almost every region, with the exception of very remote oceanic regions such as the central Pacific. On the basis of regional monthly averages, west Africa, China, and India show the highest peak monthly mean AOT value of ~0.7 at 550 nm, while the highest over-ocean aerosol loading occurs over the Mediterranean and Mid-Atlantic oceans, with a regional monthly peak of ~0.35, which is half of the peak over land. The magnitude of day-to-day variation between morning (Terra) and afternoon (Aqua) AOT varies from region to region and increases with aerosol loading for any given region. However, none of the regions examined show any consistent regional trend in morning-to-afternoon aerosol loading, all showing almost equal likelihood of increase or decrease from morning to afternoon.

Citation: Ichoku, C., L. A. Remer, and T. F. Eck (2005), Quantitative evaluation and intercomparison of morning and afternoon Moderate Resolution Imaging Spectroradiometer (MODIS) aerosol measurements from Terra and Aqua, *J. Geophys. Res.*, *110*, D10S03, doi:10.1029/2004JD004987.

1. Introduction

[2] The Moderate Resolution Imaging Spectroradiometer (MODIS) twin sensors were launched under the auspices of the NASA Earth Observing System (EOS) program: the first on 18 December 1999 aboard the Terra satellite, and the second on 4 May 2002 aboard the Aqua satellite; and have both been measuring reflected and emitted radiance from the Earth and the atmosphere, day and night. Terra and Aqua, which are both polar-orbiting satellites, cross the equator during the daytime at approximately 1030 (morning) and 1330 (afternoon) local time (LT), respectively. Radiance data are acquired by MODIS in 36 spectral bands, spanning 405–14,385 nm wavelengths, which range from the visible (VIS) through the near-infrared (NIR) and midinfrared (MIR) up to the thermal infrared (TIR) regions of the electromagnetic spectrum. They are acquired in one of three spatial resolutions at nadir: 0.25 km (bands 1–2: VIS), 0.5 km (bands 3–7: VIS-MIR), and 1 km (bands 8–36: VIS-TIR). MODIS data are being used operationally to generate a variety of geophysical parameters employed in monitoring the Earth's lands, oceans, and atmosphere. The products generated from MODIS are continuously being archived by appropriate NASA data centers and are distributed freely. The algorithms used to generate these products undergo periodic revisions, and data users are not always sure about the version and quality of the products they are using at any given time. It is, therefore, necessary to conduct periodic calibration and evaluation of the products to keep track of their evolution and make the information available to users.

[1]Science Systems and Applications Inc., Lanham, Maryland, USA.
[2]Also at Laboratory for Atmospheres, NASA Goddard Space Flight Center, Greenbelt, Maryland, USA.
[3]Laboratory for Atmospheres, NASA Goddard Space Flight Center, Greenbelt, Maryland, USA.
[4]Laboratory for Terrestrial Physics, NASA Goddard Space Flight Center, Greenbelt, Maryland, USA.
[5]Also at Goddard Earth Sciences and Technology Center, University of Maryland Baltimore County, Baltimore, Maryland, USA.

0148-0227/05/2004JD004987$09.00

[3] In this study, focus is on the MODIS aerosol products, which are retrieved at 10-km spatial resolution based on 0.25 and 0.5-km resolution reflectance data, with separate algorithms over land and ocean. The principal aerosol parameter from MODIS is the aerosol optical thickness (AOT or $\tau_{a\lambda}$) retrieved over land at 470 nm and 660 nm wavelengths (then interpolated at 550 nm), and over ocean at 550, 660, 870, 1200, 1600, and 2100 nm (then extrapolated to 470 nm). Other important MODIS aerosol parameters include the proportion (η) of AOT contributed by the aerosol fine mode fraction, Ångstrom exponent, emitted and reflected fluxes, and aerosol mass concentration, all derived over land and ocean; as well as aerosol effective radius derived over ocean only. Complete details of the original algorithms and parameters derived over land and/or ocean are given in the work of *Kaufman et al.* [1997] and *Tanré et al.* [1997], while the recent updates are described fully in the work of *Remer et al.* [2005].

[4] The purpose of evaluation, calibration, and validation is to detect biases, if any, originating from the processes involved in deriving the products, and to establish the accuracy levels of the products, based on comparison with independent observations of known accuracy (ground truth). In the case of measurement of global aerosols, the most well organized and well documented ground truth data sets are those observed under the banner of the Aerosol Robotic Network (AERONET) and other associated networks (e.g., Aeronet Canada (AEROCAN) and the French Photométrie pour le Traitement Opérationnel de Normalisation Satellitaire (PHOTONS)) [*Holben et al.*, 1998, 2001]. This network employs automatic Sun photometers/sky radiometers, which are located at over 100 sites worldwide, and whose data are regularly made available online by the AERONET team (http://aeronet.gsfc.nasa.gov/). Among other optically equivalent aerosol parameters, AOT data are derived from most AERONET Sun photometers at 340, 380, 440, 500, 670, 870, and 1020 nm wavelengths, while a few of their newer instruments also provide AOT at 532, 535, and 1640 nm. AERONET provides highly accurate AOT data, with uncertainty levels in the range of 0.01 to 0.02 (though slightly higher in the ultraviolet wavelengths) [*Eck et al.*, 1999]. Typically, AOT is measured at each AERONET site at least every 15 min during the daytime (under cloud-free conditions). It is, therefore, feasible and necessary to conduct periodic evaluation of the aerosol and other products, from both Terra and Aqua MODIS sensors, in a comparative and comprehensive manner.

[5] Results of early validation activities of the Terra-MODIS aerosol products using AERONET data were reported in the work of *Chu et al.* [2002], *Ichoku et al.* [2002], and *Remer et al.* [2002]. Subsequently, several important data filtering and algorithm improvement strategies and techniques were developed and implemented [*Gao et al.*, 2002; *Martins et al.*, 2002]. Results of some of the initial applications for global and regional studies have been published in the work of *Kaufman et al.* [2002], *Ichoku et al.* [2003], and *Levy et al.* [2003]. Indeed, the aerosol community has long begun using MODIS data quantitatively and extensively for regional and global aerosol pollution assessments, climate forcing calculations, and model comparisons [*Christopher and Zhang*, 2002; *Chu et al.*, 2003; *Yu et al.*, 2003, *Koren et al.*, 2004]. Details of the latest algorithm status and main changes, as well as longer-term validation results from Terra-MODIS have been described in the work of *Remer et al.* [2005]. Although the same aerosol algorithm is used for both Terra and Aqua MODIS processing, thus far, most of the published validation and other studies involving MODIS aerosol products used only Terra data, whereas only limited preliminary assessment has been conducted using aerosol products from Aqua MODIS [*Ichoku et al.*, 2004].

[6] In this paper, focus will be mainly on a comprehensive evaluation of Terra and Aqua MODIS spectral aerosol optical thickness $\tau_{a\lambda}$, which is the most important parameter from which others can be derived. Another major aspect of this study is to use the opportunity afforded by the availability of aerosol data from Terra and Aqua to study the patterns of aerosol distribution in the morning and afternoon. The general design and scope of the current study will be described in section 2. Updated validation activities and results of MODIS $\tau_{a\lambda}$ will be presented in section 3. A discussion of the main application-focused comparisons and synergisms between Terra and Aqua MODIS aerosol products at global, regional, and local scales will be given in section 4. The summary and conclusion will be presented in section 5.

2. Design and Scope of Study

[7] The aim of this investigation is to evaluate the quality of all available aerosol spectral optical thickness, $\tau_{a\lambda}$, generated from MODIS on both Terra and Aqua starting from the onset of data acquisition from each sensor up to the end of 2003. Obviously, this involves the analysis of a huge amount of different versions of data from two sensors covering the entire globe daily, one for almost 4 years, and the other for almost 2 years. Therefore it was necessary to design the study in such a way that the analysis will be well packaged and presented to adequately meet the needs of the scientific community, especially those involved in the quantitative use of the data.

2.1. MODIS and AERONET Aerosol Data Characteristics

[8] The calibrated radiance data from MODIS is classified as level 1B in the processing hierarchy. Algorithms are developed to retrieve geophysical parameters classified as level 2, which when aggregated (spatially, temporally, or both), can be categorized as level 3 or higher. The algorithms used for level 2 aerosol retrieval are, like all other MODIS algorithms, periodically revised and updated. After major algorithm revisions, previously processed data may be reprocessed. As a result, there could be multiple data versions (also internally referred to as data "collections") based on algorithm updates. Thus far, Terra-MODIS aerosol data has had collections 002, 003, and 004. Since collection 002 data were the first version to be generated in the operational production mode, they were basically prevalidation data and were not widely used in applications. However, collections 003 and 004 have been distributed and used quite substantially. Aqua-MODIS aerosol data started with collection 003, generated with algorithms corresponding to those of Terra-MODIS collections 003 and 004 and intervening minor updates. Aqua-MODIS collection 004 data were just starting to be produced at the time of this study, and were not yet available for

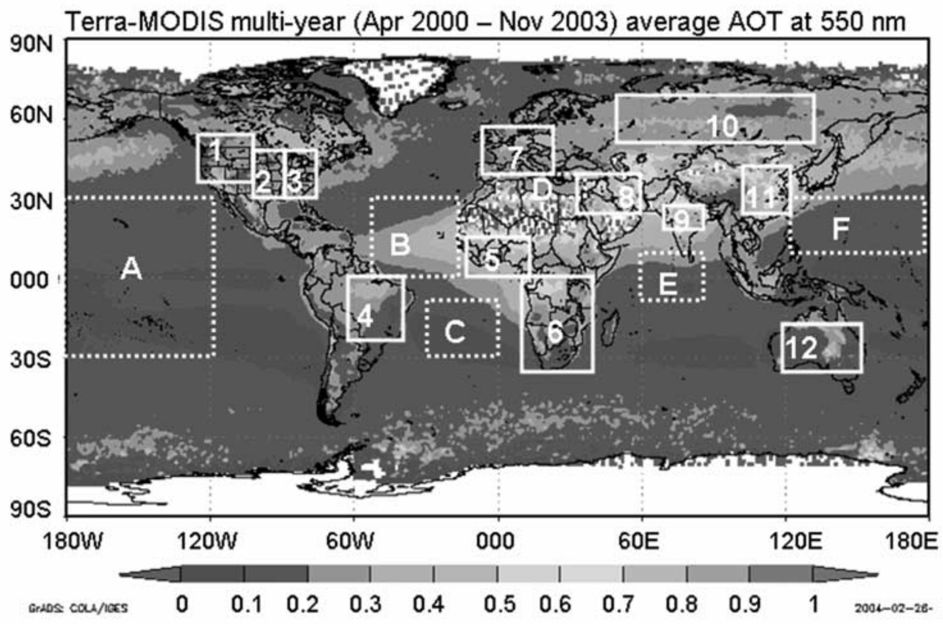

Figure 1. Multiyear (2000–2003) average aerosol optical thickness (AOT) at 550 nm wavelength from Terra-MODIS showing rectangular boundaries of various regions referenced in this study. Land regions are delimited by solid lines with numeric labels (1–12), while ocean regions are delimited by dotted lines with alphabetic labels (A–F). Since MODIS currently does not retrieve aerosols over highly bright surfaces such as Greenland, the Sahara, and the Antarctica, the purple patches (zero values) in those regions may be due to artifacts from the plotting software. See color version of this figure at back of this issue.

analysis. For simplicity in this paper, Terra-MODIS collection 003 and 004 aerosol products will be designated by Terra_V003 (or T003) and Terra_V004 (or T004) respectively, while Aqua-MODIS collection 003 products will be designated by Aqua_V003 (or A003).

[9] AERONET $\tau_{a\lambda}$ data are categorized into three levels of processing, namely: level 1.0 (aerosol data product with only predeployment instrument calibration applied), level 1.5 (cloud-screened [*Smirnov et al.*, 2000] level 1.0 data), and level 2.0 (quality assured level 1.5 data, having been checked and adjusted with predevelopment and postdeployment calibrations). AERONET level 1.5 data are available in near real time, while, depending on site and length of deployment, level 2.0 is only available several weeks to several months behind real time. Therefore, for reasons of expediency, MODIS aerosol validation is performed mostly with AERONET level 1.5 data.

[10] In evaluating MODIS aerosol products with AERONET in certain parts of this paper, the adopted convention for comparison is to subtract AERONET data from corresponding MODIS data and use the resulting "MODIS-AERONET" (or M-A) difference to assess the performance of MODIS relative to AERONET. This has been done such that, taking AERONET to be the ground truth, "positive" and "negative" values of these M-A differences will respectively represent "over-estimation" and "under-estimation" by MODIS.

2.2. Geographic Considerations of Study

[11] Although part of the analysis will be conducted in an integral global fashion, however, given the variability of aerosol regimes, such an analysis alone may not be sufficiently effective in communicating the data quality assessment results. Therefore, to enable a better assessment of regional peculiarities, several large regions were identified such that the study could also be conducted in a comparative way between them. Twelve rectangular regions were selected over land, and six over ocean. Since this work is somewhat driven by evaluation/validation of different aerosol types with AERONET measurements, the distribution of these regions was determined by two factors, namely (1) the main distribution centers of different aerosol types and (2) availability of AERONET stations.

[12] Figure 1 shows a map of multiyear average AOT at 550 nm for the period of April 2000 to November 2003, derived from Terra-MODIS global monthly average data sets at 1° spatial resolution. The map was generated using the MODIS Online Visualization and Analysis System (MOVAS), which can be used online at (http://lake.nascom.nasa.gov/movas/). The boundaries of the rectangular regions selected for this study are shown in white; with solid lines for land and dotted lines for ocean. The land regions are labeled with numerals (1 to 12), while the ocean regions are labeled with alphabets (A to F). Table 1 shows the correspondence between the labels and the names of the regions shown in Figure 1, as well as coordinates of the box boundaries and the dominant aerosol types in each region. The dominant aerosol type in each region has been determined from literature [*Holben et al.*, 2001; *Dubovik et al.*, 2002; *Kaufman et al.*, 2002; *Ichoku et al.*, 2004; *Remer et al.*, 2005]. "Mixed" is used to designate aerosol types with more than two dominant species (such as combined

Table 1. Regions Selected for This Study, As Shown in Figure 1, With Corresponding Boundary Coordinates and Dominant Aerosol Types

Label	Name	Min_Lon	Max_Lon	Min_Lat	Max_Lat	Aerosol_Type
				Land		
1	NW_America	−125	−110	40	60	smoke
2	US_Central	−110	−90	30	50	mixed
3	US_East	−90	−70	30	50	urban/industrial pollution
4	Brazil	−60	−40	−25	0	smoke
5	W_Africa	−15	15	0	15	mixed
6	S_Africa	10	40	−35	0	smoke (some dust, urban/ind)
7	W_Europe	−10	30	40	60	urban/industrial pollution
8	Middle_E	30	60	20	40	dust
9	India	70	85	20	30	mixed
10	Russia	50	140	50	70	smoke
11	China	100	120	25	45	mixed
12	Australia	120	150	−35	−15	mixed
				Ocean		
A	C_Pacific	−180	−120	−30	30	oceanic
B	M_Atlantic	−50	−15	0	30	dust/smoke
C	S_Atlantic	−30	10	−30	0	smoke (some dust)
D	Medit_Sea	0	35	30	40	mixed
E	N_Indian	60	90	−10	10	pollution/dust
F	Asian_Pacific	120	180	0	40	mixed

influence of urban/industrial pollution, smoke, and dust). Most of the regional studies performed in this paper will refer to the regions represented in Figure 1 and Table 1. To facilitate broad zoning in later sections, all regions having at least a negative (-ve) boundary longitude (Min_Lon or Max_Lon) in Table 1 will be classified as Western Hemisphere (WH), while others will be classified as Eastern Hemisphere (EH).

3. MODIS Aerosol Data Validation

[13] The validation of MODIS aerosol products is accomplished mainly with the use of equivalent data acquired from the ground based AERONET network. Collocated MODIS and AERONET data are extracted and compared in order to evaluate MODIS accuracy based on that of AERONET, either globally, regionally, or locally. The principle of MODIS and AERONET data sampling were described in detail in the work of *Ichoku et al.* [2002]. However, for completeness in this paper, the process will be summarized in subsection 3.1.

3.1. MODIS and AERONET Data Sampling for Validation

[14] The main difficulty in data sampling from MODIS and AERONET is the differences in their data structures. During each overpass, MODIS covers an extensive area across a given AERONET instrument site almost in an instant, whereas the AERONET Sun photometer takes point measurements several times during the daytime. Therefore, whereas MODIS data expresses spatial variability, AERONET data expresses temporal variability. To reconcile these differences in order to achieve a balanced comparison, spatial averages of MODIS pixels falling within a 50 × 50 km box centered over each AERONET station are taken to compare with temporal averages of AERONET data measured ±30 min of MODIS overpass time. This equivalence is based on the assumption that, from estimates of Saharan dust transport, air masses transporting aerosol travel a distance of approximately 50 km per hour on the average [*Ichoku et al.*, 2002]. Thus, if a segment of an aerosol plume is imaged by MODIS within a 50 × 50 km box centered over an AERONET station, it is assumed that part of that aerosol plume segment may have passed over the AERONET station during the 30 min preceding MODIS overpass, while the other part will pass over the station during the 30 min following MODIS overpass. As such, the MODIS and AERONET statistics derived as described here are indeed determined from different samples of the same aerosol population. These MODIS validation statistics are generated quasi-operationally as the MODIS level 2 aerosol products are being produced. One of the conditions adopted for validation with the spatiotemporal averages computed here is that the MODIS statistics would have been computed with at least 5 pixels (out of a maximum of 25 pixels expected in a 50 × 50 km box) and AERONET statistics would have been computed with at least 2 observations (out of a maximum of 5 observations expected in a period of 1 hour of observations at 15 min time intervals) [*Ichoku et al.*, 2002; *Remer et al.*, 2002].

[15] To verify the quality of AERONET level 1.5 $\tau_{a\lambda}$ data for aerosol validation relative to the corresponding level 2.0 (quality assured) data, the AERONET level 1.5 AOT ±30 min averages for 2000 to 2003 were plotted against corresponding AERONET level 2.0 data at three wavelengths (440, 670, and 870 nm), separately over land and ocean and for Terra and Aqua overpass times. In all cases, there was almost perfect correlation, with coefficient of determination (r^2) ranging from 0.993 to 1, thereby making the correlation coefficients (r) practically always equal to unity. Given this impressive correlation between AERONET levels 1.5 and 2.0 data sets, our confidence is reassured that it is valid to use AERONET level 1.5 $\tau_{a\lambda}$ to validate MODIS $\tau_{a\lambda}$. Nevertheless, it is pertinent to note that, when AERONET level 2.0 data are not available, any errors that may exist in level 1.5 would have no effect, since in a correlation analysis, only points having both data types contribute. In this study, during the evaluation

analysis, effort will be made to exclude specific level 1.5 AERONET data known to be unsuitable for validation. That filtering process will be discussed in section 3.2.

[16] MODIS and AERONET wavelengths do not match exactly except at 870 nm. Therefore, to enable comparison at matching wavelengths, AERONET $\tau_{a\lambda}$ used for MODIS validation at 470, 550, and 660 nm are interpolated from AERONET $\tau_{a\lambda}$ at 440 and 870 nm, based on the assumption of uniform spectral dependence between these two wavelengths, represented by the Ångstrom exponent, α, parameter (equation (1)):

$$\alpha_{870/440} = \frac{\ln(\tau_{a870}/\tau_{a440})}{\ln(870/440)}, \quad (1)$$

where, $\alpha_{870/440}$ is the Ångstrom exponent based on AOT at 440 and 870 nm wavelengths.

3.2. Evaluation of MODIS Data Accuracy With AERONET

[17] An important aspect of the preparation activities embarked upon prior to the launch of the first MODIS, was an experimental determination of the range of uncertainties expected from MODIS aerosol retrieval, which for $\tau_{a\lambda}$ were estimated to be $\pm(0.05 + 0.2\ \tau_{a\lambda})$ over land and $\pm(0.03 + 0.05\ \tau_{a\lambda})$ over ocean [*Kaufman et al.*, 1997; *Tanré et al.*, 1997]. In each case, the constant term represents the estimated error due to surface reflectance assumptions, while the second term, which is often proportional to $\tau_{a\lambda}$, represents the error due to aerosol model assumptions. The uncertainty in surface reflectance and model assumptions are, obviously, both expected to be larger for land than for ocean. Nevertheless, earlier validation results showed that most of the over-land and over-ocean Terra-MODIS $\tau_{a\lambda}$ data met their respective prespecified expectations [*Chu et al.*, 2002; *Remer et al.*, 2002, 2005].

3.2.1. Data Assessment and Filtering

[18] In this work, the first step in the evaluation of the MODIS $\tau_{a\lambda}$ with corresponding AERONET level 1.5 data involved computing the relative errors for all collocated data points to determine the %pass of MODIS $\tau_{a\lambda}$ (percentage falling within the expected uncertainty) at each AERONET station, in order to identify possible station-specific effects on MODIS performance. Tables 2a and 2b list respectively the land and ocean AERONET stations where less than 50% of MODIS τ_{a550} fall within the expected uncertainty; showing the average number of collocated data points (*n* data) and the average %pass (averaged from T003, T004, and A003). A careful examination of the site characteristics enabled the compilation of the probable reasons, why there was such low MODIS/AERONET agreement over each of such stations. The main site-dependent sources of uncertainties over pure land sites include: uncertainty in surface reflectance assumptions due to the attenuating effects of excessive surface brightness (usually associated with semi-arid and arid regions), urban surface variability, and snow and melting snow in the higher latitudes. All ocean-based AERONET instruments exist on coastal or island locations, with the exception of a few instruments on offshore platforms, which are close to land. Therefore the main factors affecting ocean sites also affect coastal and island sites, and include: uncertainty in distinguishing land from water especially when the coastline is complex, as well as the attenuating effects of sandy beaches, swamps, marshes, water sediments, and sea ice (in higher latitudes) on measured reflectance. Factors, which can be common to land and ocean sites (coastal or not) include: persistent cloud cover, and possible error in AERONET data due to instrument or other operational problems, and AERONET observation from high altitude mountain peaks not accounting for the lower level aerosols measured by MODIS in the surrounding areas. Furthermore, although collocated samples of MODIS and AERONET used to derive the spatiotemporal averages are assumed to represent the same aerosol population over any given site, differences in the special distribution of aerosol loading can affect the MODIS/AERONET agreement substantially.

[19] In certain situations, AERONET/MODIS collocated data sets are known to be either not properly matched or to contain errors, and the integrity of the evaluation can be compromised by the use of such data. Therefore, although it is practically impossible to identify all such cases, attempt has been made to exclude from the AERONET/MODIS comparisons conducted in this paper those known to fall under such categories. The excluded stations are identified by footnote b in Tables 2a and 2b. The excluded stations are not necessarily those that exhibit the least %pass. Rather, the following criteria are used for exclusion both over land and ocean: data for periods where AERONET data were known to be erroneous (Ilorin, 25 April to 30 August 2003; Kejimkujik), stations where AERONET instruments are located at very high altitudes (Mauna-Loa), and stations with less than 3 collocated pairs. In this last case (<3 pairs), they are assumed to be either new or temporary stations where the measurement may not be sufficiently characterized, or long-term stations with perpetual (cloud or instrument) problems limiting data acquisition times, with the probability that even the measured data may be contaminated. In addition, over land, offshore stations (COVE, Helgoland, and Venise) are excluded, because it is known that any land within the MODIS 50 $\times$ 50 km box would be marginal, while over ocean, stations known to be located far from actual ocean (Bac_Lieu and CEILAP-BA) are also excluded. Although, many of the other stations may also fall under these categories, they have not been excluded because these unfavorable characteristics were not confirmed in their case.

3.2.2. Integrated Global Evaluation

[20] When the MODIS aerosol products were of limited volume and only from Terra, the evaluation or validation was based on the use of standard scatterplots for regional or global data [*Chu et al.*, 2002; *Ichoku et al.*, 2002; *Remer et al.*, 2002]. The second round of Terra-MODIS validation was conducted with a larger volume of data (two year's worth), and the standard scatterplots were no longer applicable directly. Instead, the data were first aggregated according to value ranges before use in modified scatterplots [*Ichoku et al.*, 2004; *Remer et al.*, 2005]. Given that the data volume has continued to increase, with the addition of Aqua-MODIS and multiple data versions, only the modified scatterplots can be used to graphically express the global correlation in a reasonable way.

[21] The data aggregation process for the generation of modified scatterplots involved the binning of AERONET

Table 2a. Over-Land AERONET Sites Where MODIS Shows Less Than 50% Rate of Falling Within Error Bounds and Probable Causes[a]

Name	*n* Data	Pass, %	Probable Cause(s) of Elevated Uncertainty
Arica	9	0	urban site, bordering on the Atacama desert, extremely arid
Bac_Lieu	8	0	swampy river delta (0% pass over ocean)
Barrow	16	13	snow and melting snow problem
Beijing	69	39	urban surface variability; mixed aerosol types
Bratts_Lake	74	16	prairie; glacial terrain; dotted by pothole lakes
Brookhaven	43	35	on New York Long Island: some water, and sandy beaches
Carpentras	126	46	located in the foothills of mountains
CCNY	60	32	New York City urban surface variability
CEILAP-BA	94	36	Buenos Aires urban surface variability, nearness to wide river delta
Chen-Kung_Univ	7	38	uncertainty in data sampling, urban with adjacent mountains
Chulalongkorn	7	31	Bangkok, Thailand, urban surface variability; instrument on high rise building
Churchill	13	0	tundra vegetation, snow, ice
Coconut_Island	24	29	island site with mountains nearby, cloudy
Coleambally	40	48	arid area of Australia
Corcoran	83	38	site in the irrigated central valley of California, with nearby lakes
COVE[b]	57	20	offshore platform, only limited land strip: swampy or sandy
CRYSTAL_FACE[b]	1	0	coastal Florida with swamps and sandy beaches
Dhabi[b]	1	0	very arid coastal site
Dunkerque	30	37	coastal site and urban surface variability
El_Arenosillo	211	25	sandy soil with pine trees, nearby marshes
ETNA	9	22	AERONET instrument on slope of high mountain, not total column aerosol
Etosha_Pan	10	37	extremely arid and bright salt pan
Evora	56	16	?
FORTH_CRETE	134	20	semiarid
Fresno	117	47	located in a region with irrigated agricultural valleys and mountains
GISS	68	39	New York City urban surface variability
Gotland	120	44	snow and melting snow problem, coastal
Guadeloup	11	16	suspected AERONET instrument problem (some time periods)
Halifax	79	34	snow and melting snow problem; coastal harbor, with possible floating ice
Helgoland[b]	5	31	North Sea offshore platform, nearby land is small and rocky island; ice, snow, melting snow
Ilorin[b]	35	33	known AERONET instrument problem (25 Apr. to 30 Aug. 2003)
ISDGM_CNR	129	21	venise urban surface variability, water canals
Kejimkujik[b]	11	26	AERONET instrument problem, clouds
La_Jolla	69	35	urban and sandy beach
Lake_Argyle	77	3	semiarid, station near lake
Lanai	69	30	island surrounded by ocean, limited land surface, which is semiarid
Longyearbyen	20	33	very high latitude; Ice, sea ice, snow, and melting snow problem
Maricopa	144	6	site in irrigated fields adjacent to arid bright surfaces
Mauna_Loa[b]	136	43	high altitude ($\sim$3.4 km), not total column aerosol
MISR-JPL	10	23	urban surface variability and mountainous altitude variability
Nes_Ziona	124	18	semiarid
Oyster	6	0	swampy land and sandy beach (100% pass over ocean)
Palencia	41	31	?
Pic_du_midi	21	47	high-altitude station, not total column aerosol
Railroad_Valley	135	31	arid, dry lake bed
Rimrock	111	44	prairie, canyon, agricultural, semi-arid area
Rogers_Dry_Lake	106	24	arid, dry lake bed
Saturn_Island	90	48	land surrounded by water
Sevilleta	160	35	arid
Shelton[b]	2	0	site near the multichannel Platte River in Nebraska
Sua_Pan	6	27	arid, dry lake bed; bright salt pan
TABLE_MOUNTAIN_CA	31	2	AERONET instrument on mountain (2.2 km altitude) near Mojave desert; not total column aerosol
THALA	66	35	AERONET instrument at 1.1 km altitude in a mountainous arid region; not total column aerosol
Toulon	45	28	urban surface variability; marshy water-logged surroundings, with neighboring hills
Toulouse	142	39	urban surface variability
Tucson	18	0	arid and urban surface variability
Venise[b]	187	16	offshore platform; only limited land strip with venise urban surface variability and canal
Wallops	119	35	marshes, sandy beaches
White_Sands	18	14	dry lake bed, gypsum flakes bright surface
Yulin	41	48	urban surface variability; also semiarid, bordering the Mu Us desert

[a]A question mark (?) in the probable cause column indicates "not known." There were a total of 175 land AERONET sites involved in this study. Sites indicated with "yes" in the first column are completely excluded from MODIS validation analysis because of known site-specific problems not related to MODIS retrieval.

[b]Excluded data.

Table 2b. Over-Ocean AERONET Sites Where MODIS Shows Less Than 50% Rate of Falling Within Error Bounds and Probable Causes[a]

Name	*n* Data	Pass, %	Probable Cause(s) of Elevated Uncertainty
Anmyon	11	41	possible water sediment in the Yellow Sea
Arica	46	37	cloudy in the morning
Bac_Lieu[b]	2	0	swampy river delta (also 0% pass over land); ∼10 km from ocean
BORDEAUX	6	41	busy sea port
Bragansa[b]	2	0	known AERONET instrument problem
CEILAP-BA[b]	10	7	near Buenos Aires; close to mouth of a wide river turning to estuary with sediments; far from ocean
Che-Ju	17	22	very mixed aerosol type (dust, pollution, sea salt)
Chen-Kung_Univ	3	0	uncertain data sampling
Dakar	40	45	dust nonsphericity problem
ETNA	3	40	high-altitude station, not total column aerosol
Dhabi	5	40	water is not open ocean; UAE Persian Gulf; complex coastline, possible land masking inaccuracy
Guadeloup	17	33	suspected AERONET instrument problem (some time periods)
IMS-METU-ERDEMLI	65	49	complex coastline, possible land masking inaccuracy
Mauna_Loa[b]	32	6	high altitude (∼3.4 km), not total column aerosol
Mont_Joli	10	40	water is not open ocean, just St Lawrence River; possible land masking inaccuracy
NCU_Taiwan	7	29	uncertain data sampling
Norfolk_State_Univ	8	38	complex coastline, possible land masking inaccuracy
Oostende	34	43	busy sea port
Rome_Tor_Vergata	10	40	AERONET instrument far from ocean
Shirahama	34	47	complex coastline, possible land masking inaccuracy
Taipei_CWB	3	0	uncertain data sampling
UCLA[b]	1	0	AERONET instrument far from ocean

[a]A question mark (?) in the probable cause column indicates "not known." There were a total of 56 ocean AERONET sites involved in this study. Sites indicated with "yesy" in the first column are completely excluded from MODIS validation analysis because of known site-specific problems not related to MODIS retrieval.
[b]Excluded data.

$\tau_{a\lambda}$, with a uniform class interval of 0.05. For each class, the statistics of all MODIS data points corresponding to the AERONET data points in that class are calculated to represent the MODIS $\tau_{a\lambda}$ for that class. Figure 2 shows modified scatterplots of MODIS $\tau_{a\lambda}$ class averages against AERONET $\tau_{a\lambda}$ bin center values, separately for T003, T004, and A003, at 470, 550 and 660 nm wavelengths over land, and at 550, 660, and 870 nm over ocean. Only MODIS $\tau_{a\lambda}$ averages computed from at least 3 data points were plotted. The MODIS $\tau_{a\lambda}$ standard deviations are plotted as error bars only for the 550-nm curves (to limit clutter). The dotted diagonal line in each panel is the 1-to-1 line, while the near-diagonal pair of broken lines defines the prespecified uncertainty envelop {land: $\pm(0.05 + 0.2\ \tau_{a\lambda})$, or ocean: $\pm(0.03 + 0.05\ \tau_{a\lambda})$}, which is invariably wider for land than for ocean. The total number of data points (*np*) used is shown in each graph, while the cumulative counts of data points in each class are plotted at all wavelengths represented. The percent proportion of MODIS τ_{a550} falling within the specified uncertainty bounds in each class are plotted (%pass_550). Over land, MODIS tends to overestimate slightly at low AOT values ($\tau_{a550} < 0.15$ for T003, and $\tau_{a550} < 0.25$ for T004 and A003), with ∼60% falling within the uncertainty bounds; but more (∼75%) of the individual collocated MODIS retrievals fall within the uncertainty range at moderate aerosol loading; while for the largest AOT values (constituting less than 2% of total retrievals), there is wide fluctuation (probably because the statistics were based on very small samples, with greater spatial and temporal variation in AOT). At low AOT values, the error bars are shorter and the %pass_550 range is larger (∼65%) for T003 relative to T004 and A003, probably because of increased uncertainty due to extension of retrieval over brighter surfaces [*Remer et al.*, 2005] in the newer versions (T004 and A003). Over ocean, there is no significant offset at the lowest AOT values, and despite the more stringent error tolerance, most of the MODIS $\tau_{a\lambda}$ class averages fall within the uncertainty boundaries, except at 870 nm where there seems to be slight underestimation for the largest 5% of the AOT values, probably due to uncertainty in the representation of nonsphericity in the dust model [*Remer et al.*, 2005]. Indeed, whereas the %pass_550 exceeds 80% at the lowest AOT values for all the data versions, %pass_550 decreases continuously as the AOT values increase, and fluctuates very widely for the largest AOT values (less than 2% of total retrievals).

[22] To obtain an overall quantitative summary of how well MODIS $\tau_{a\lambda}$ data meet the uncertainty expectations and correlate with AERONET $\tau_{a\lambda}$ globally, the percentages of MODIS $\tau_{a\lambda}$ within the uncertainty envelopes and the correlation parameters were computed from the actual (unbinned) MODIS and AERONET $\tau_{a\lambda}$ collocated pairs, for each data set (T003, T004, and A003) over land and ocean, separately using AERONET levels 1.5 and 2.0. Table 3 shows the number of data point pairs N used for computing the parameters for each data set (T003, T004, and A003) and the values of the parameters at different wavelengths. The parameters include: percentages of MODIS $\tau_{a\lambda}$ within the uncertainty bounds (%pass), the linear correlation coefficients r, and the slopes and intercepts of the regression lines. Referring to results based on AERONET level 1.5, T003 has larger %pass (more data contained within the error bounds) both over land and ocean, and has better r and intercept over land, thereby supporting the theory that the extension of retrieval over brighter surfaces in the later algorithm versions (T004 and A003) introduced greater uncertainty over land (as evidenced by the size of the error bars in the plots of

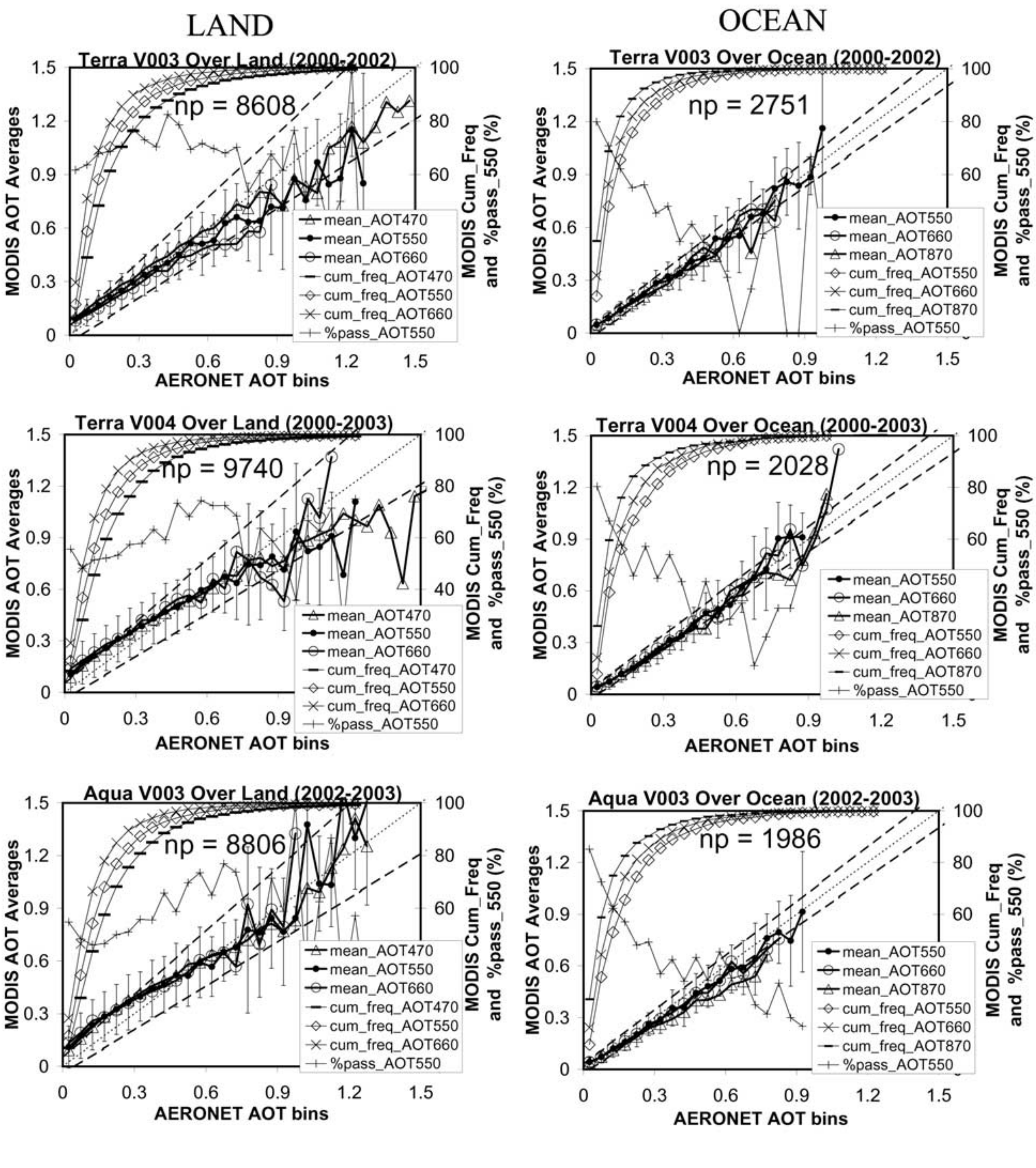

Figure 2. Modified scatterplots of MODIS global class average AOT (based on collocated AERONET AOT bins) against the AERONET AOT bin center values for T003, T004, and A003 over land (at 470, 550, 660 nm wavelengths) and ocean (at 550, 660, 870 nm wavelengths). The standard deviations of the AOT classes for MODIS are shown as error bars only for the 550 nm curves (to limit clutter). The dotted diagonal line is the 1-to-1 line, while the pair of near diagonal broken lines are the bounds of the uncertainty envelops. The total number of data points (*np*) used in each data group is shown on each panel, while the cumulative counts of data points in each class are plotted at all wavelengths represented. The percent proportion of MODIS AOT at 550 nm falling within the specified uncertainty bounds in each class are plotted (%pass_550). See color version of this figure at back of this issue.

Figure 2). Over ocean, T004 and A003 are better than T003 in terms of *r*, slope and intercept; showing that the later algorithm versions (T004 and A003) produced overall improvement over ocean. The fact that %pass is slightly worse in these later versions may have been caused by differences in the distribution of aerosol types and loading. There appears to be no significant difference, in regards to %pass, for using AERONET level 1.5 or 2.0. This is

Table 3. Parameters of the Global Accuracy Ratio (% pass) and Linear Regression Fit of 50 × 50 km Average MODIS Level 2 AOT Against ±30 min Average AERONET Levels 1.5 and 2.0 AOT

Data Version	N	λ = 470 nm	λ = 550 nm	λ = 660 nm	λ = 870 nm
		Level 1.5 AOT: Percent of Data Within Error Bounds (% Pass)			
T003_Land	8608	58.8	67.3	70.2	N/A[a]
T004_Land	9740	53.8	53.5	52.8	N/A
A003_Land	8806	48.1	50.8	51.0	N/A
T003_Ocean	2751	56.3	62.2	65.6	69.6
T004_Ocean	2028	49.7	57.0	62.4	66.7
A003_Ocean	1986	54.5	59.3	63.1	67.4
		Level 1.5 AOT: Linear Correlation Coefficient (r)			
T003_Land		0.81	0.76	0.62	N/A
T004_Land		0.76	0.68	0.51	N/A
A003_Land		0.76	0.68	0.51	N/A
T003_Ocean		0.83	0.81	0.78	0.74
T004_Ocean		0.92	0.93	0.93	0.93
A003_Ocean		0.92	0.92	0.93	0.92
		Level 1.5 AOT: Slope of Regression Line			
T003_Land		0.75	0.66	0.55	N/A
T004_Land		0.73	0.72	0.70	N/A
A003_Land		0.84	0.75	0.66	N/A
T003_Ocean		0.78	0.74	0.70	0.59
T004_Ocean		1.07	1.04	1.01	0.93
A003_Ocean		0.96	0.92	0.89	0.79
		Level 1.5 AOT: Intercept of Regression Line			
T003_Land		0.107	0.092	0.086	N/A
T004_Land		0.122	0.128	0.141	N/A
A003_Land		0.120	0.136	0.154	N/A
T003_Ocean		0.048	0.045	0.047	0.047
T004_Ocean		−0.024	−0.016	−0.004	0.007
A003_Ocean		0.002	0.002	0.007	0.013
		Level 2.0 AOT: Percent of Data Within Error Bounds (% Pass)			
T003_Land	7252	58.3	67.5	70.7	N/A
T004_Land	3550	52.9	55.0	56.5	N/A
A003_Land	2787	48.8	55.5	56.8	N/A
T003_Ocean	2402	57.6	63.3	66.7	70.6
T004_Ocean	670	53.3	59.4	66.0	69.2
A003_Ocean	611	57.4	62.2	66.3	71.2
		Level 2.0 AOT: Linear Correlation Coefficient (r)			
T003_Land		0.85	0.82	0.71	N/A
T004_Land		0.80	0.71	0.52	N/A
A003_Land		0.85	0.81	0.66	N/A
T003_Ocean		0.91	0.91	0.91	0.89
T004_Ocean		0.93	0.94	0.95	0.96
A003_Ocean		0.92	0.92	0.92	0.92
		Level 2.0 AOT: Slope of Regression Line			
T003_Land		0.79	0.75	0.69	N/A
T004_Land		0.76	0.78	0.79	N/A
A003_Land		1.01	0.92	0.83	N/A
T003_Ocean		0.95	0.96	0.97	0.89
T004_Ocean		1.01	1.00	0.99	0.94
A003_Ocean		0.91	0.89	0.88	0.80
		Level 2.0 AOT: Intercept of Regression Line			
T003_Land		0.100	0.078	0.066	N/A
T004_Land		0.113	0.111	0.117	N/A
A003_Land		0.067	0.081	0.094	N/A
T003_Ocean		0.017	0.014	0.015	0.019
T004_Ocean		−0.006	−0.005	0.001	0.007
A003_Ocean		0.013	0.011	0.013	0.015

[a]N/A, not applicable because the land data do not have the 870 nm wavelength.

because the act of filtering out a few erroneous AERONET level 1.5 $\tau_{a\lambda}$ to level 2.0 has very little effect on the %pass parameter, which is a simple ratio between two large numbers. However, the use of AERONET level 2.0 $\tau_{a\lambda}$ appears to yield appreciable improvement in the correlation coefficient *r*, slope, and intercept of the regression line, both over land and ocean, especially for T003, which, being the oldest data set, has the largest proportion of available

AERONET level 2.0 $\tau_{a\lambda}$. This improvement shows that MODIS $\tau_{a\lambda}$ data are intrinsically more accurate than they appear to be when validated with the readily available level 1.5 AERONET data, as is often the case.

[23] In summary, based on point-by-point comparison with AERONET, the proportion of MODIS-retrieved AOT falling within the specified uncertainly envelope globally ranges from approximately 50% to 70%, generally increasing with wavelength from 470 to 870 nm, both over land and ocean (see Table 3). However, over land, when based on $\tau_{a\lambda}$ bin averages (as Figure 2 shows), at low aerosol loading (approximately, $\tau_{a550} < 0.20$) MODIS has the tendency to over estimate slightly, at moderate aerosol loading (approximately, $0.20 < \tau_{a550} < 0.70$) MODIS measures more accurately, while for very heavy aerosol loading (approximately, $\tau_{a550} > 0.70$) MODIS accuracy fluctuates unpredictably, with more tendency to underestimation. Over ocean, at low aerosol loading (approximately $\tau_{a550} < 0.20$) MODIS retrieves $\tau_{a\lambda}$ mostly accurately. The accuracy of MODIS retrieval over ocean decreases as aerosol loading increases, although considering that the over-ocean uncertainty tolerance is very stringent and that more than 90% of the cases have relatively low AOT ($\tau_{a550} <$ 0.40, as seen with the aid of the cumulative frequency curves in Figure 2), the net accuracy is very high. Overall, by comparing the parameters of the equivalent versions of Terra (T004) and Aqua (A003) $\tau_{a\lambda}$, there does not appear to be any clear difference in performance between them.

3.2.3. Time-Varying Regional Evaluation

[24] The aim of this study is not limited to validation for the globe or a specific targeted region based on prespecified error criteria, but one of the main objectives is to assess the general accuracy of the aerosol products from both Terra and Aqua MODIS in a manner that will be of direct benefit to the user of the products for various applications including long-term climate studies [*Remer et al.*, 2005]. Therefore effort is made to integrate the stationary, regional, and temporal aspects of this analysis in such a simple way as to enable the user to calculate the level of error potentially involved in using data from the available versions of Terra- or Aqua-MODIS products for a given region and time period. As such, the M-A differences of AOT at 550 nm ($\Delta^{M\text{-}A}\tau_{a550}$) calculated with AERONET level 1.5 data over all sites were grouped into regions, and their regional monthly averages were calculated. Time series plots were generated for these monthly averaged $\Delta^{M\text{-}A}\tau_{a550}$ values and plotted over the corresponding MODIS average AOT at 550 nm for the different data versions and regions, as shown in Figures 3a and 3b. The condition for plotting a data point is that its monthly average must have been computed from at least 3 values. For each region, the upper sets of curves represent the regional monthly average $\Delta^{M\text{-}A}\tau_{a550}$, showing whether MODIS agrees with, overestimates, or underestimates AERONET, and by how much; while the lower sets of curves are corresponding time series of the MODIS regional monthly average τ_{a550}, which serve as reference, showing where the levels of disagreement may depend on the AOT level.

[25] The large data gaps in some regions is because some have only one or just a few AERONET stations, and due to the preponderance of cloudy situations in some regions, it is difficult to obtain the required two AERONET observations within ±30 min of MODIS overpass. Thus some of the monthly averages plotted in Figures 3a and 3b were computed from only one station and perhaps just a few days, which are certainly not representative of the situation for the region or for the month. In such cases, the errors may appear exaggerated with respect to what a true average derived from a representative sample set would be. However, where qualifying data were found for only a single AERONET station in a given region, the name of that station is shown in the graph.

[26] Figure 4 shows the overall regional average bar chart for the evaluation of MODIS τ_{a550} with AERONET level 1.5 τ_{a550}. The bars represent the average MODIS τ_{a550} for each data set (T003, T004, and A003) for the entire period of collocated data availability for this study, while the topping spikes are the corresponding average $\Delta^{M\text{-}A}\tau_{a550}$, which, depending on whether they project above or below the top of the bars, represent MODIS overestimation or underestimation respectively, with respect to AERONET. Tables 4a and 4b show the overall summary of the regional validation over land and ocean, respectively, with the list of AERONET stations whose data were available for this study, and an outline of results for each region based on Figures 3a, 3b, and 4. The generalizations, which can be made from these results include: (1) the over-ocean retrievals show better agreement with AERONET than the over-land retrievals; (2) for the same satellite and data version there are significant differences in performance between regions; (3) over ocean, there is little or no difference in performance between T003, T004, and A003 for a given region; (4) over land, average $\Delta^{M\text{-}A}\tau_{a550}$ for T003 is generally smaller than those of T004 and A003, which show identical performance because the algorithms used in retrieving T004 and A003 were almost identical; (5) regardless of satellite or data version, regions with tendency toward overestimation are all over land and include: northwest America, central United States, eastern United States, western Europe, and India (with an overall average overestimation of the order of 0.05), and China, Middle East, and Australia (with an overall average overestimation of the order of 0.15).

3.3. Apportionment of Errors in MODIS Aerosol Data Products

[27] A wide variety of checks and verifications are conducted during the development and revisions of MODIS algorithms before they are implemented in the production mode. Nevertheless, given that there are several other factors, which can affect the quality of the products, including sensor calibration, satellite motion and observation geometry, environmental conditions (such as cloud cover or surface brightness and variability) during measurement, ancillary data accuracy, model assumptions, and even unforeseen errors in the algorithm, which may not be obvious in a few test cases, it is important to conduct postproduction bulk data checks with a much larger volume of data, particularly with respect to an independent set of measurements such as AERONET data, with a view to identifying the main sources of errors and developing strategies to correct them.

[28] To identify the main sources of errors in the MODIS aerosol products, the individual (not the monthly mean)

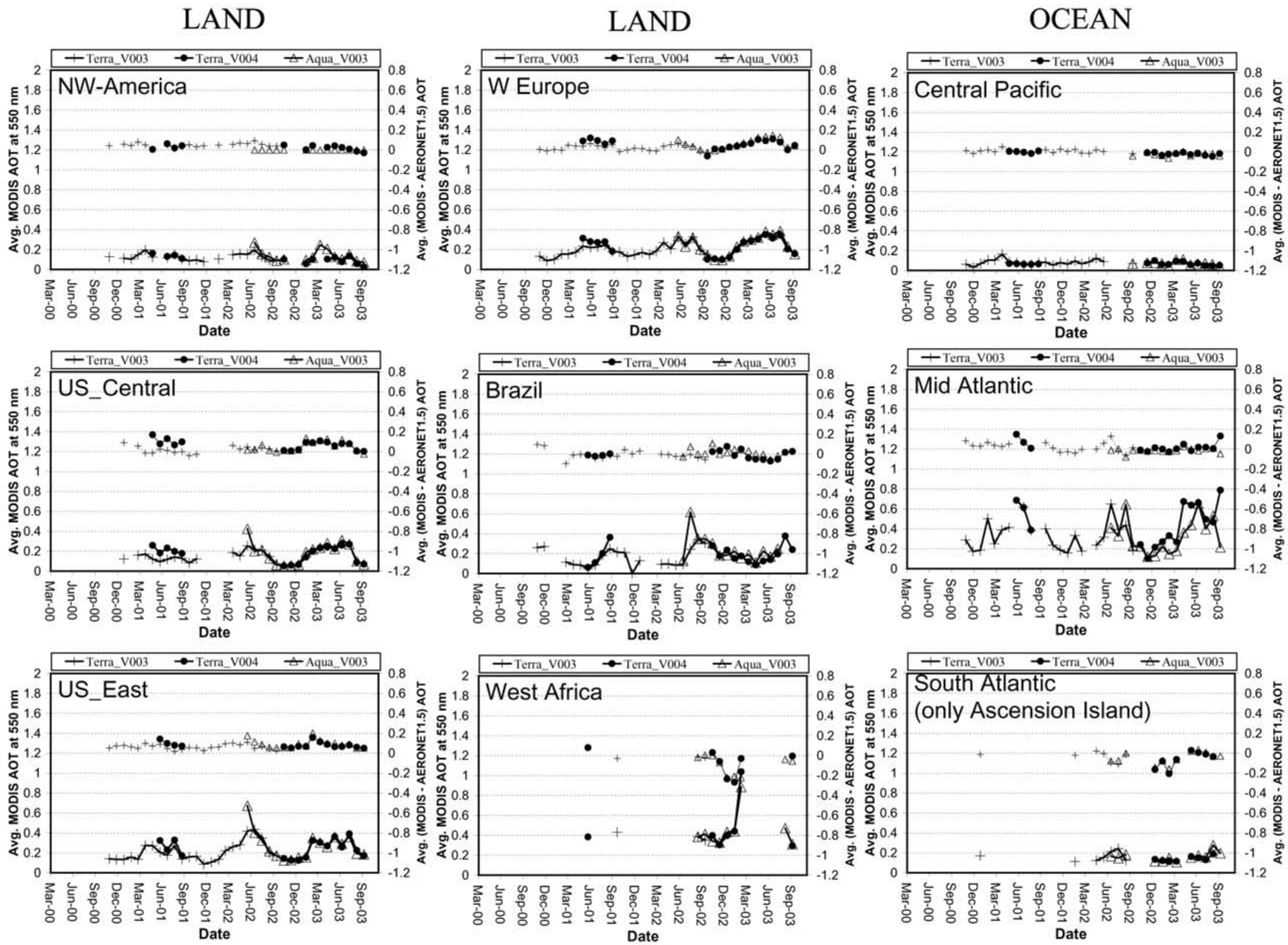

Figure 3a. Western Hemisphere time series of regional monthly mean AOT at 550 nm and corresponding (MODIS-AERONET) differences for the different MODIS aerosol data versions (T003, T004, and A003). See color version of this figure at back of this issue.

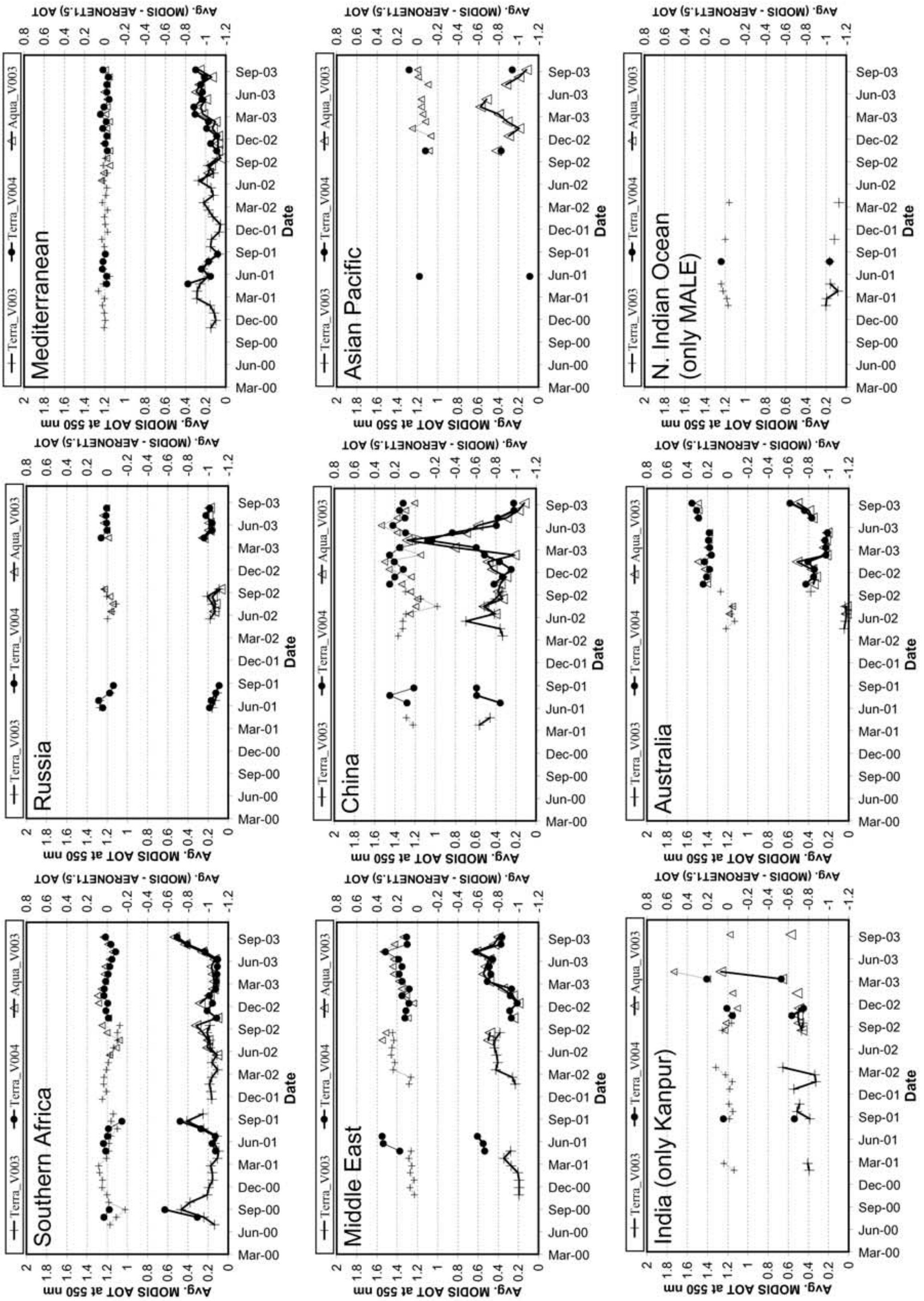

Figure 3b. Eastern Hemisphere time series of regional monthly mean AOT at 550 nm and corresponding (MODIS-AERONET) differences for the different MODIS aerosol data versions (T003, T004, and A003). See color version of this figure at back of this issue.

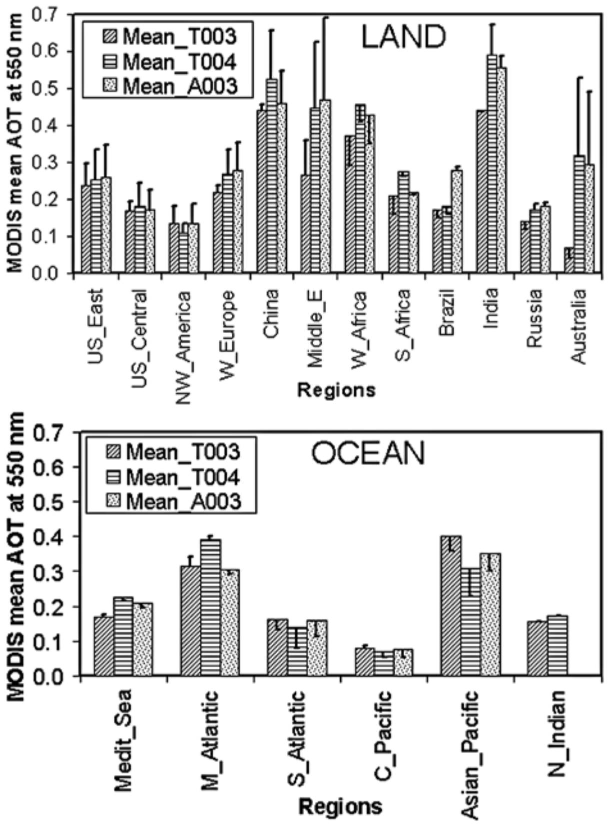

Figure 4. Summary of regional comparison of MODIS AOT at 550 nm with AERONET level 1.5 AOT. The bars represent the overall regional averages computed from the MODIS 50 × 50 km local averages over AERONET stations for the entire period of each data set (T003, T004, or A003). The topping spikes are the corresponding average MODIS-AERONET differences and represent MODIS overestimation or underestimation with respect to AERONET depending on whether they project above or below the top of the bar.

values of $\Delta^{M-A}\tau_{a550}$ were directly plotted against different parameters including water vapor and satellite observation geometry parameters in order to investigate possible influences by these parameters. Plots generated against water vapor did not show any major trends or biases. Patterns observed with respect to scattering angle (which incorporates solar zenith and azimuth angles and the sensor zenith and azimuth angles) are different over land and ocean, but there is no obvious dependence on scattering angle. However, plots against the sensor zenith angle, which is directly proportional to scan angle, clearly portrays some dependence.

[29] Figure 5 shows plots of $\Delta^{M-A}\tau_{a550}$ class means against sensor zenith angle bins (5° class intervals), representing the different versions of MODIS aerosol products (T003, T004 and A003) for land and ocean. The class standard deviations are represented as error bars, shown only for the Land_T004 and Ocean_T004 to avoid clutter. Overall, there are larger deviations over land than over ocean, because MODIS aerosol products are generally more accurate over ocean [*Remer et al.*, 2005]. The over-land curves are definitely inclined; being more positively biased at lower scan angles, with gradual descent toward the zero line at larger scan angles. Similar analysis conducted on regional basis show that regions with brighter surfaces (Middle East, Australia, US_Central) or regions with numerous small water bodies or more physical development (US_East, west Europe) show more scan angle dependence than regions with darker or more uniform surfaces (Brazil, Russia, southern Africa). This apparent overestimation by MODIS at smaller scan angles is probably caused by the dominance of the effects of land surface variability [*Chu et al.*, 2002; *Ichoku et al.*, 2002], which diminishes as one moves away from nadir. In an independent study on the role of "adjacency effect" on aerosol remote sensing, it was observed that "contrast of surface scene is the most important factor affecting the accuracy of aerosol retrieval" and "at subkilometer resolution the error of aerosol retrieval due to adjacency effect diminishes for higher off nadir angles" [*Lyapustin and Kaufman*, 2001, p. 11,913]. Although MODIS aerosol products are reported at 10-km spatial resolution, they are retrieved from the 0.25-km and 0.50-km resolution radiance channels. A recent study revealed that the omission of polarized radiative transfer in over-land aerosol retrieval introduces errors in AOT, which can reach up to 0.3 in extreme cases, and can be negative or positive depending on the scattering geometry, but is negligible at nadir and increases with both solar and sensor zenith angles [*Levy et al.*, 2004]. Therefore the obvious positive bias at small sensor zenith angle over land cannot be due to the polarization effect, but most likely due to surface effects. The over-ocean curves show almost no inclination, but show a slight increase of (both negative and positive) deviations at very high scan angles. This increase of deviation at very high scan angles may also be present in the over-land data, but may have been obscured by the surface effects.

4. Terra and Aqua Comparison and Synergism

[30] MODIS aerosol products are applicable to various types of aerosol studies. Globally and regionally, they can be used to develop aerosol climatology and calculate radiative forcing effects on climate. Locally, they can be used to assess pollution levels and effects on environmental dynamics. The fact that MODIS acquires data both in the morning (Terra) and afternoon (Aqua) makes the data set particularly strategic for studies involving some diurnal variability assessment, although with average overpass time difference of only ~3 hours (Terra = >1030, Aqua = >1330 LT), the full diurnal pattern cannot be characterized.

[31] In this section, emphasis will be focused on the relationships and differences between morning (Terra) and afternoon (Aqua) observations, without distinguishing data versions. The Terra data versions (T003 and T004) are not differentiated in this segment of the analysis because, as Figures 3a and 3b shows, in the data sets used for this research, during the period of availability of A003, there is no overlap between T003 and T004. Thus combination of the later two, allows for data continuity to match A003 for an appreciable time period. Also, since the focus in this section is "morning" and "afternoon" rather than version differences, and the accuracy of data versions is not significantly different, there is no need to differentiate T003 and

Table 4a. Summary of the Regional Validation of MODIS AOT With AERONET Over Land

Label	Region Name	AERONET Stations Used	MODIS Validation Summary
1	northwest America	HJAndrews, Lochiel, Missoula, Rimrock, Saturn_Island	MODIS shows slight to moderate overestimation; T003 and A003 have the same accuracy; T004 has better accuracy than the others
2	central United States	BRSN_BAO_Boulder, Cart_Site, Chequamegon, IHOP_Homestead, KONZA_EDC, Sevilleta, Sioux_Falls, White_Sands	MODIS shows slight to moderate overestimation; T004 became more overestimated than T003 because the algorithm for T004 included retrieval over brighter surfaces, which cause overestimation; T004 and A003 show comparable accuracies
3	eastern United States	Big_Meadows, BONDVILLE, Brookhaven, CARTEL, CCNY, Columbia_SC, Egbert, GISS, GSFC, Harvard_Forest, MD_Science_Center, Norfolk_State_Univ, Oyster, Penn_State_Univ, Philadelphia, Rochester, SERC, Stennis_Walker_Branch, Wallops	MODIS shows moderate overestimation; T004 is slightly more overestimated than T003 because more bright surfaces were included in the retrieval for T004 than for T003; T004 and A003 show comparable accuracies
4	Brazil	Alta_Floresta, Balbina, Belterra, CUIABA-MIRANDA, Sao_Paulo, Sao_Paulo_State_Park	there is some balance in negative and positive error distribution for all product versions; the errors are small, with Terra (T003 and T004) showing a net underestimation, and Aqua (A003) the opposite
5	west Africa	Banizoumbou, Ilorin, Ougadougou	this region shows moderate underestimation (irrespective of satellite or version), probably because its mix of pollution, smoke, dust, and high cloudiness, causes over-filtering of clouds in MODIS
6	South Africa	Bethlehem, Etosha_Pan, Inhaca, Kaoma, Maun_Tower, Mongu, Mwinilunga, Ndola, Pietersburg, Senanga, Skukuza, Solwezi, Sua_Pan, Zambezi	this region shows slight bias toward underestimation, which was moderate with T003, but improved drastically for T004 and A003 because of the adjustment of the single scattering albedo for southern African smoke, which has greater absorption relative to other regions
7	western Europe	Avignon, Belsk, BORDEAUX, Bucarest, Creteil, Davos, Fontainebleau, Gerlitzen, Gotland, Hamburg, IFT_Leipzig, ISDGM_CNR, Ispra, Lille, Minsk, Modena, Moldova, Munich_Maisach, Oostende, Palaiseau, Pic_du_midi, Rome_Tor_Vergata, Sopot, Tarbes_Etal, The_Hague, Toravere, Toulouse, Villefranche	MODIS seems to be accurate in periods with low to moderate AOT, but overestimates moderately during the summer peak pollution seasons; overall, T004 and A003 are more overestimated when compared with T003 because of the effect of the inclusion of brighter surfaces in the later (T004 and A003) retrievals
8	Middle East	IMS_METU_ERDEMLI, Nes_Ziona	MODIS appears to overestimate always because the area is mostly bright surfaces; the moderate overestimation with T003 increased to high with T004 and A003 because of the inclusion of even brighter surfaces
9	India	Kanpur	only one AERONET station is located in this region, with only few monthly averages; not representative of region; however, there is little to moderate net overestimation overall
10	Russia	Krasnoyarsk, Tomsk	only two AERONET stations and few monthly averages; there appears to be a good accuracy here for all the data sets
11	China	Beijing, Dalanzadgad, Yulin	MODIS appears to overestimate always because the area is mostly bright surfaces with complex aerosol mix, but overestimation increased with T004 and A003 because of the inclusion of even brighter surfaces
12	Australia	Coleambally, Lake_Argyle	Australian AERONET stations are relatively new and may still be uncalibrated, thereby causing the overestimation by MODIS due to bright surfaces to appear constantly increasing

Table 4b. Summary of the Regional Validation of MODIS AOT With AERONET Over Ocean

Label	Region Name	AERONET Stations Used	MODIS Validation Summary
A	central Pacific	Coconut_Island, Lanai, Midway_Island, Tahiti	MODIS shows high accuracy here, with T004 and A003 slightly underestimated
B	Mid-Atlantic	Capo_Verde, Dahkla, Dakar	the accuracy here is surprisingly good, given that this region is affected by a mix of smoke, dust, and sea salt; however, Terra-MODIS (T003 and T004) shows slight over-estimation, and Aqua-MODIS (A003) the opposite
C	South Atlantic	Ascension_Island	only one AERONET station is located here; not representative of region; however, net result is little to moderate underestimation
D	Mediterranean Sea	ETNA, FORTH_CRETE, IMC_Oristano, IMS-METU-ERDEMLI, Lampedusa, Nes_Ziona	MODIS always shows high accuracy here regardless of product version; this is very impressive
E	northern Indian	MALE	only one AERONET station; very limited data sets; no collocated data from Aqua; however, available Terra data seem excellent
F	Asian Pacific	Anmyon, Che-Ju, Chen-Kung_Univ, Nauru, NCU_Taiwan, Noto, Okinawa, Shirahama, Taipei_CWB	data were limited in this region; mostly moderate underestimation for all data versions; underestimation probably due to aerosol mixing

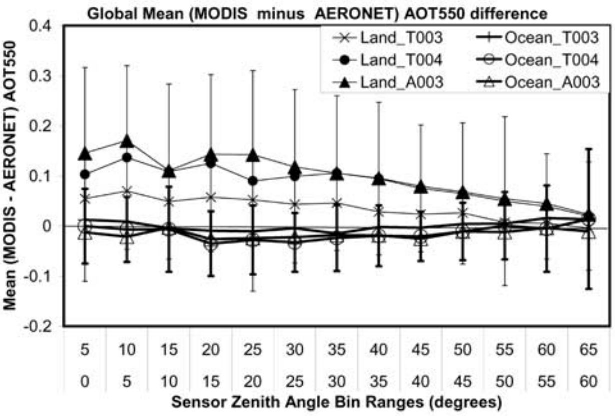

Figure 5. Plots of global mean (MODIS-AERONET) differences of AOT at 550 nm, grouped according to sensor zenith angle bins (5° intervals), for different Terra and Aqua MODIS data versions (T003, T004, and A003) over land (thin lines) and ocean (thick lines), plotted against their respective sensor zenith angle bins. Error bars (shown only for the land and ocean T004 to limit clutter) are the corresponding standard deviations. See color version of this figure at back of this issue.

T004 for this part of the analysis. Therefore, in the following subsections, all reference to Terra (or morning) will be based on T003 and T004 combined, while references to Aqua (or afternoon) will be based on A003 only.

4.1. Global Aerosol Abundance From Terra and Aqua MODIS

[32] The analysis in this subsection is based on data acquired only over AERONET stations, which spatially does not represent full global sampling. In a study conducted with AERONET data just before the launch of the first MODIS on Terra, *Kaufman et al.* [2000] posed the question: "Will aerosol measurements from Terra and Aqua polar orbiting satellites represent the daily aerosol abundance and properties?" This question was addressed in that paper, where AERONET data segments observed at predicted Terra and Aqua overpass times were used to represent MODIS observations, and the conclusion was that "Terra and Aqua aerosol measurements can represent the average annual value to within 2% error" [*Kaufman et al.*, 2000, p. 3861]. However, now that actual MODIS data are available, it will be interesting to see if they will reproduce the pattern that AERONET predicted. To do this, average AOT at 470, 550, and 660 nm were calculated from the collocated MODIS/AERONET (50 × 50 km and ±30 min) validation data, separately for MODIS and AERONET, at Terra and Aqua overpass times, over land and ocean. Prior to averaging, Ångstrom exponent (α) was computed from all AERONET data as defined in equation (1), and AERONET AOT were interpolated at 470, 550, and 660 nm. Then, all data sets were partitioned into three groups on the basis of the range of AERONET Ångstrom exponents (α) that they fall into ($\alpha < 0.7$, $0.7 < \alpha < 1.8$, or $\alpha > 1.8$). *Kaufman et al.* [2000] indicated that $\alpha < 0.7$ would represent predominantly dust aerosols (large size mode), $\alpha > 1.8$ predominantly pollution or smoke aerosols (small size mode), and $0.7 < \alpha < 1.8$ mixed continental aerosols (medium size range). It should be noted that α was derived by *Kaufman et al.* [2000] using 865 and 550 nm wavelengths, whereas the pair used in this work were 870 and 440 nm because these are the two AERONET wavelengths spanning the three wavelengths (470, 550, 660 nm) upon which this analysis is based.

[33] Figure 6 shows the wavelength-dependent plots of the AOT averages from MODIS and AERONET data for the three divisions of Ångstrom exponents, separately at Terra and Aqua overpass times, over land and ocean (Figures 6a–6d). One aspect that needs to be highlighted from these global average spectral AOT ($\tau_{a\lambda}$) plots is that, for each α division, considering morning (Terra) and afternoon (Aqua) observations separately, over-land values are markedly higher than their over-ocean counterparts; whereas when over-land and over-ocean plots are considered separately, afternoon (Aqua) average values are slightly higher than corresponding morning (Terra) values. Over land, MODIS overestimates AERONET in all three α divisions, although the difference is least at the $\alpha < 0.7$ division, and less for Terra than for Aqua in the other two divisions. Also, average spectral dependencies from MODIS are not very consistent with those of corresponding AERONET divisions. Over ocean, MODIS and AERONET $\tau_{a\lambda}$ are quite close, but their spectral dependencies are noticeably different, especially for the coarse particle size (dust and sea salt) category ($\alpha < 0.7$). However, when the overall average $\tau_{a\lambda}$ for the three α divisions are calculated and plotted without distinguishing Terra and Aqua or land and ocean (Figure 6e), MODIS is seen to overestimate AERONET by about 0.03 (for the coarse mode dominated aerosol) to 0.06 (for the fine mode dominated aerosol). Therefore, since the global average $\tau_{a\lambda}$ estimated from AERONET at Terra and Aqua overpass times represented the AERONET global daily aerosol abundance accurately [*Kaufman et al.*, 2000], it follows from this analysis that MODIS would overestimate the global average $\tau_{a\lambda}$ by about 0.03 to 0.06, which indeed correspond approximately to MODIS detection limit over land and ocean, based on the prespecified accuracy ranges of $\pm(0.05 + 0.2\,\tau_{a\lambda})$ over land and $\pm(0.03 + 0.05\,\tau_{a\lambda})$ over ocean [*Kaufman et al.*, 1997; *Tanré et al.*, 1997; *Chu et al.*, 2002; *Remer et al.*, 2002, 2005]. It is pertinent to note, however, that most of the data used in this analysis comes from land, where most AERONET stations are located, whereas most MODIS aerosol retrievals are over ocean, which are much more accurate, implying that fully sampled MODIS global averages would represent the reality much more accurately than the above analysis shows.

[34] To assess the seasonal trends, if any, in the observed MODIS overestimate relative to AERONET, monthly averages of the collocated AOT at 550 nm were derived and plotted for the three divisions of Ångstrom exponent considered ($\alpha < 0.7$, $0.7 < \alpha < 1.8$, or $\alpha > 1.8$). Figure 7 shows separate time series plots of these averages for Terra and Aqua overpass times, over land and ocean. MODIS and AERONET curves are designated with M(α_range) and A(α_range), respectively. Over land, MODIS shows a systematic overestimation with respect to AERONET in all three groups both at Terra and Aqua overpass times, almost all the time. However, in the large mode ($\alpha < 0.7$)

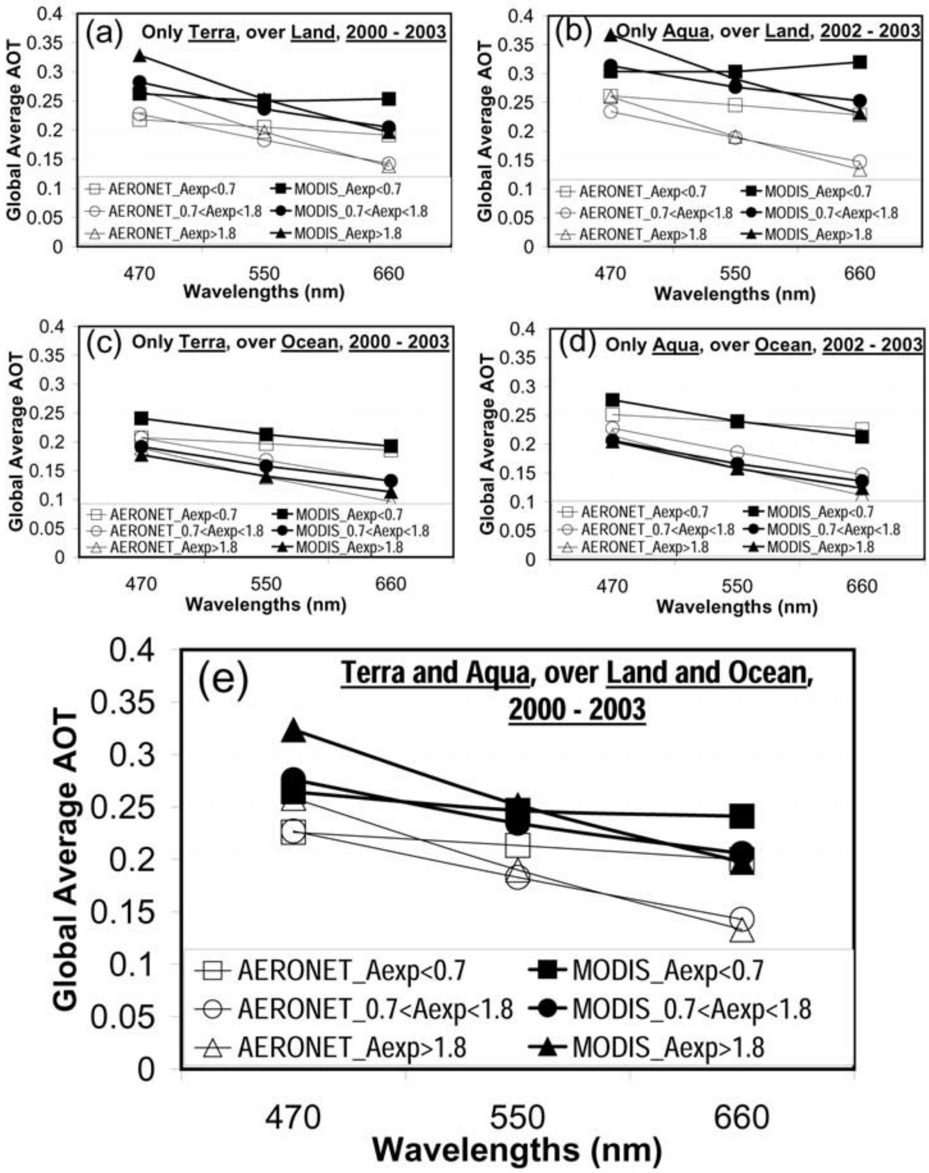

Figure 6. Spectral plots of the 3-year (2000–2003) overall average aerosol optical thickness (AOT) from MODIS and AERONET, computed from collocated local averages (MODIS: 50 × 50 km, AERONET: +30 min), partitioned according to three AERONET Ångstrom exponent ranges (Aexp < 0.7, 0.7 < Aexp < 1.8, or Aexp > 1.8). The plots are shown (a–d) separately and (e) combined for Terra and Aqua overpass times over land and ocean.

division, AERONET shows higher values than MODIS during some peak (probably dust) events, particularly in the fall season of 2001 and 2003. Over ocean, there is very good agreement between MODIS and AERONET for all three α divisions on both Terra and Aqua, although again the large mode ($\alpha < 0.7$) shows MODIS slightly overestimating AERONET occasionally. One remarkable feature of all curves put together is the seasonality in global concentration of all the aerosol size groups, both in the morning (Terra) and afternoon (Aqua), over land and ocean; with the peak periods being usually around boreal spring to summer, while the troughs are mostly in boreal winter. Also, considering only the Terra plots, which show longer-term data, there seems to be a net gradual increase in aerosol loading during the three year period shown (November 2000 to November 2003). In particular, over ocean, during that time period, the net large mode ($\alpha < 0.7$) loading (probably dust) seems to have almost doubled, both from MODIS and AERONET data, at least in the morning (at Terra overpass time). It is important to specify that the foregoing net increase is based on data acquired only over AERONET stations, and may not represent the full global aerosol trend.

4.2. Regional Seasonal and Diurnal Aerosol Trends From MODIS

[35] Although the global seasonal and diurnal trends of τ_{a550} have been discussed in the preceding subsection,

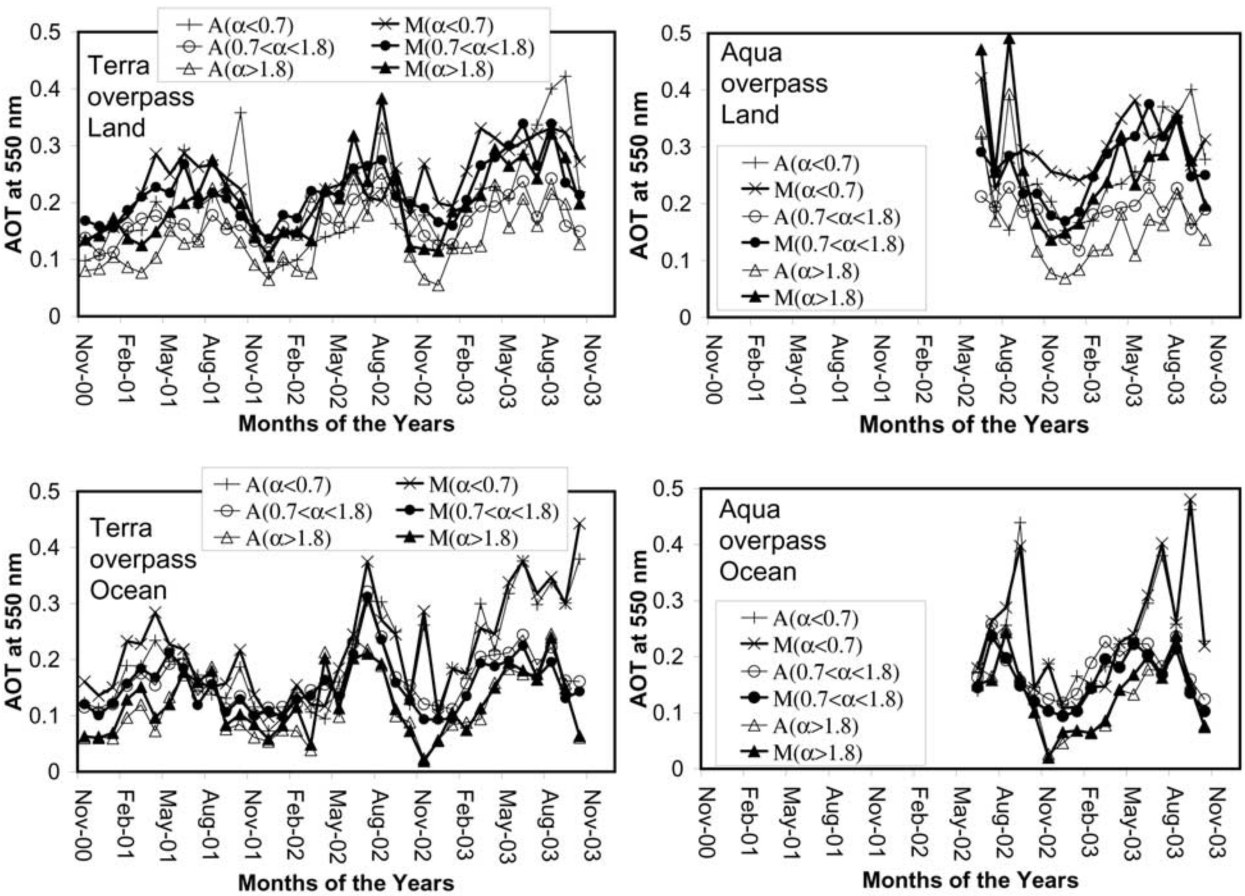

Figure 7. Monthly mean aerosol optical thickness (AOT) from MODIS and AERONET for the overpass times of Terra and Aqua over land and ocean. The averages were computed from local means (MODIS: 50 × 50 km; AERONET: ±30 min) over all AERONET stations grouped according to three ranges of AERONET Ångstrom exponent ($\alpha < 0.7$, $0.7 < \alpha < 1.8$, or $\alpha > 1.8$). See color version of this figure at back of this issue.

nevertheless, it is useful to see the differences between the regions (as designated in Figure 1). To achieve a balanced analysis, it is preferable to use regional averages based on full data sampling for each region, as opposed to the use of averages based on just samples taken over a few discrete (AERONET) stations. Therefore, in this section, only regional daily and monthly τ_{a550} averages, derived from all pixels of the daily MODIS level 2 (10-km resolution) aerosol data within each region will be used.

[36] Figure 8 shows the time series of the Terra-MODIS monthly average τ_{a550} plotted for each of the regions, roughly separated into Western Hemisphere (WH) land (top panel), Eastern Hemisphere (EH) land (middle panel), and ocean (bottom panel). Note that the vertical scale of the ocean panel is twice that of the land plots. With the exception of the central Pacific, which shows almost no variation over time, all other regions (land and ocean alike) portray moderate to very strong seasonal cycles, although the specific peak and low seasons vary from region to region. Among the WH land regions, west Africa shows by far the highest aerosol loading, with the level of τ_{a550} at its low season generally higher than the maxima over the rest of the Western Hemisphere regions. This dominance of west Africa is probably because it is situated within the equatorial African biomass-burning belt and is in close proximity to the southern African smoke and Saharan dust source regions. Therefore it is almost continuously impacted by large volumes of smoke and dust, as well as other aerosols originating from local sources. China and India, both of which top the list in the EH land, are subjected to similar heavy impacts of dust, smoke, and pollution. The regional monthly mean τ_{a550} range (low-to-peak) for these three regions is approximately 0.3 to 0.7. The Middle East, which experiences high aerosol loading during its intense dust (spring-summer) seasons, settles to very moderate levels in winter, with a range of ~0.2 to 0.6. The major biomass burning regions: Brazil, Russia, and southern Africa have comparable but moderate seasonal peak levels, with a range of ~0.1 to 0.4. The industrialized regions of west Europe and North American (NW_America, US_Central, and US_East) have not only the same aerosol loading, but also follow the same spring-summer high to winter low seasonal cycle, with a range of ~0.1 to 0.3, although NW_America is the least typical. Australia shows a range of ~0.1 to 0.25. Over ocean, the Mediterranean

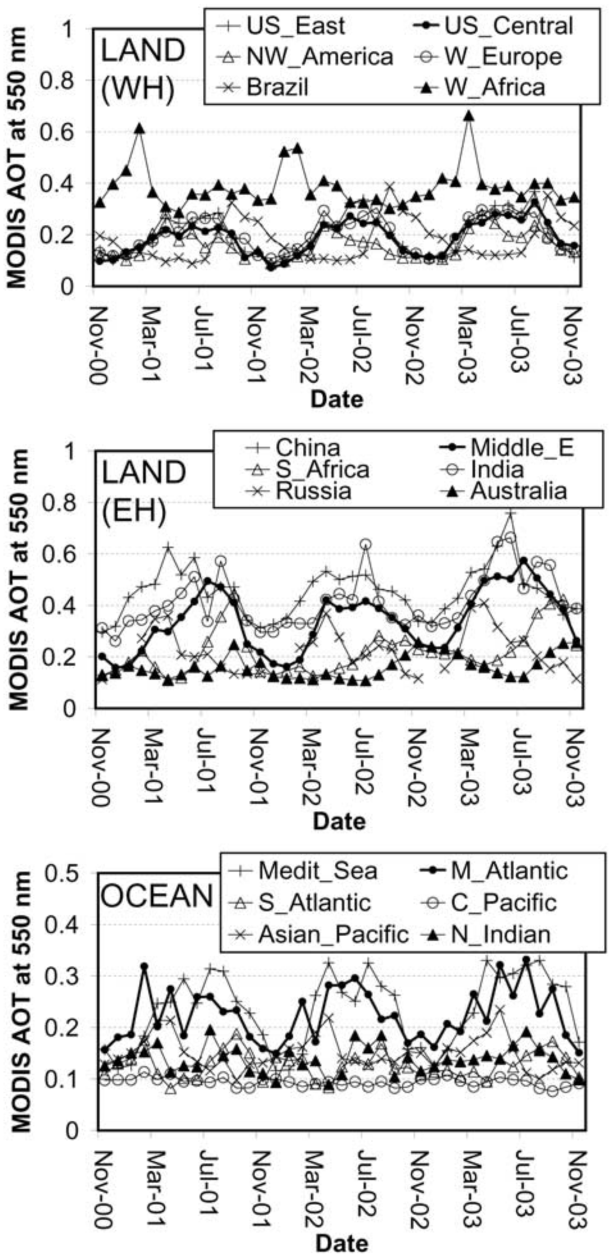

Figure 8. Time series of regional monthly average AOT at 550 nm, derived directly from MODIS level 2 (10-km resolution) daily aerosol products. The regions are grouped as (top) Western Hemisphere (WH) land, (middle) Eastern Hemisphere (EH) land, and (bottom) ocean. Note that the scale of the ocean panel is twice that of the land plots. See color version of this figure at back of this issue.

Sea and the Mid-Atlantic Ocean, because of their nearness to Saharan dust sources, dominate over other oceanic regions, and have approximately the same level of aerosol loading and seasonal cycle, with a range of ~0.15 to 0.35. Therefore the regional monthly mean τ_{a550} range over these two most heavily loaded oceanic regions is about half that of the most heavily loaded land regions (west Africa, China, and India). The Asian Pacific Ocean reflects the impact of Asian continental dust and biomass burning, with a range of ~0.15 to 0.25, while the southern Atlantic and north Indian Oceans display the effects of their nearness to southern African smoke and Indian mixed aerosol regions respectively, with a range of ~0.1 to 0.2. Central Pacific remains the overall cleanest region with a low and slim range of ~0.08 to 0.12, because it is the most remote of all regions from land where the major aerosol sources are located. It is pertinent to mention that the dust-dominated regions in Figure 8 do not show the type of increasing trend seen in Figure 7 (for the dust category) probably because Figure 8 plots are based on MODIS full spatial sampling (as opposed to just over AERONET sites) and include all aerosol types and size ranges in each region (as opposed to just the large particle group).

[37] Knowledge of the diurnal variation of aerosol loading is very important in many areas of application and, using AERONET data, *Smirnov et al.* [2002] showed that major urban/industrial centers exhibit the greatest diurnal cycle, with a variation of 10–40% during the day at most sites. Although the twice-a-day aerosol observation offered by MODIS (~1030 and 1330 LT) may not allow full characterization of the diurnal patterns in aerosol loading, however, the morning-to-afternoon variation for each region can be examined using the differences between the Terra (morning) and Aqua (afternoon) regional daily τ_{a550} averages. Figures 9a and 9b show the time series plots of the Terra-MODIS daily average τ_{a550} (lower points, left scale) coplotted with the corresponding (Aqua-Terra) τ_{a550} differences (upper points, right scale) for each of the study regions. These regional daily mean (Aqua-Terra) τ_{a550} differences will be denoted by $D^{A-T}\tau_{a550}$ for convenience in the rest of this section. Terra is subtracted from Aqua, such that positive and negative differences will represent morning-to-afternoon increase and decrease, respectively. The plots cover the period of coexistence of Terra and Aqua (June 2002 to November 2003) within the period of this study (February 2000 to November 2003). Table 5 shows the overall average of the $D^{A-T}\tau_{a550}$ values plotted in Figures 9a and 9b for each region for the entire time period represented. These overall average regional (Aqua-Terra) difference of AOT at 550 nm will, for easy reference, be designated by $Avg^{A-T}\tau_{a550}$, in the rest of this discussion. One feature that needs to be pointed out in Figures 9a and 9b is the enhanced positively biased differences in the plots for NW_America, US_Central, US-East, and Russia in February/March 2003, which resulted in the elevation of the overall mean $Avg^{A-T}\tau_{a550}$ for these regions ($0.018 < Avg^{A-T}\tau_{a550} < 0.063$). This situation was caused by melting snow contamination in Aqua-MODIS, whose cloud/snow mask was initially inadequate until it was corrected after that season. Other than that known situation, surprisingly, the $D^{A-T}\tau_{a550}$

Figure 9a. Western Hemisphere time series of regional daily average Terra-MODIS AOT at 550 nm (lower points, left scale) coplotted with the corresponding (Aqua-Terra) τ_{a550} differences (upper points, right scale). The regional averages were derived directly from MODIS level 2 (10-km resolution) aerosol data from Terra and Aqua before the (Aqua-Terra) τ_{a550} daily differences $D^{A-T}\tau_{a550}$ were calculated.

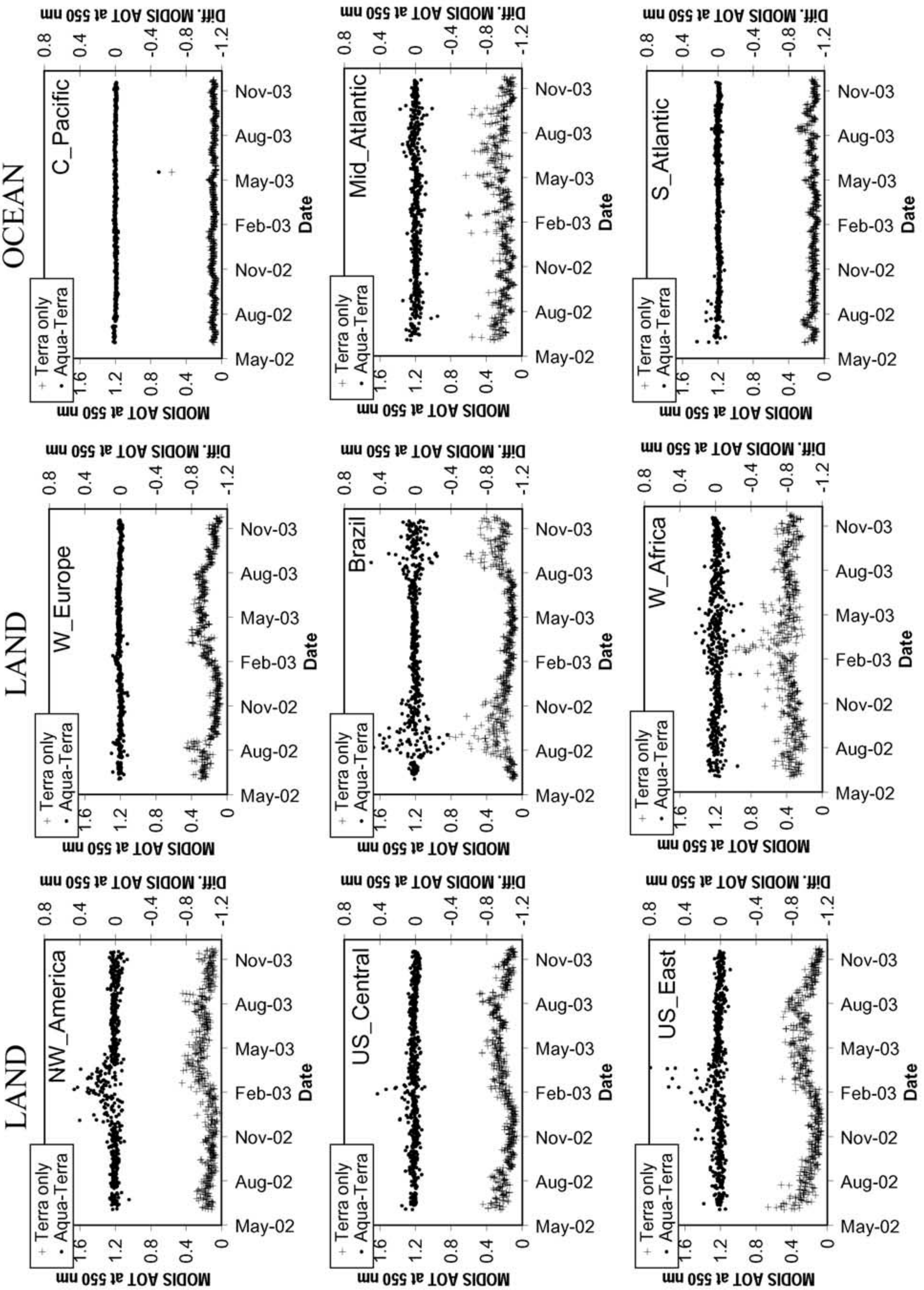
OCEAN
C_Pacific
Mid_Atlantic
S_Atlantic
LAND
W_Europe
Brazil
W_Africa
LAND
NW_America
US_Central
US_East
Terra only
Aqua-Terra
MODIS AOT at 550 nm
Diff. MODIS AOT at 550 nm
Date
May-02
Aug-02
Nov-02
Feb-03
May-03
Aug-03
Nov-03

Figure 9a

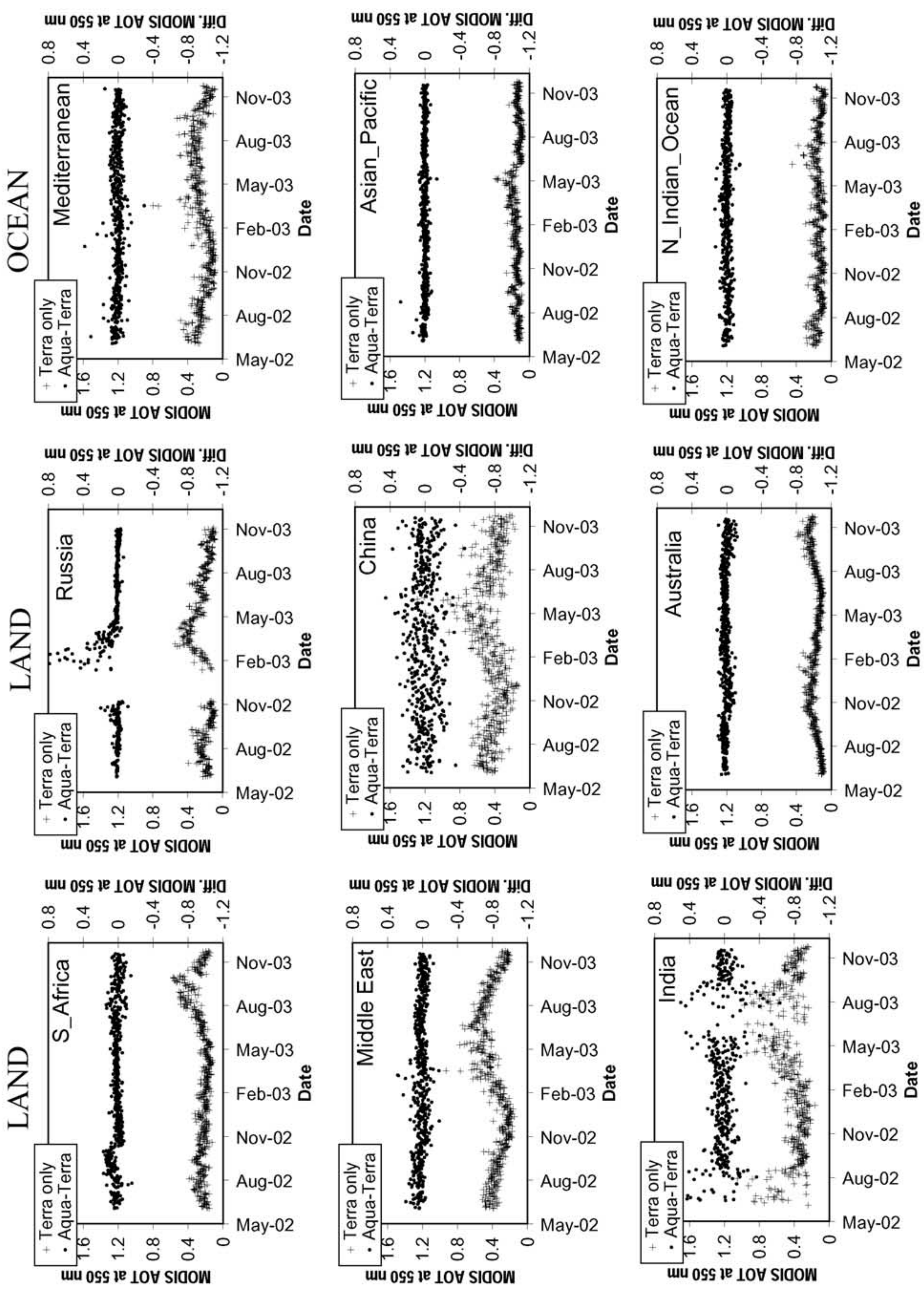
LAND
LAND
OCEAN
S_Africa
Russia
Mediterranean
Middle East
China
Asian_Pacific
India
Australia
N_Indian_Ocean
+ Terra only
• Aqua-Terra
MODIS AOT at 550 nm
Diff. MODIS AOT at 550 nm
Date
May-02
Aug-02
Nov-02
Feb-03
May-03
Aug-03
Nov-03

Figure 9b

Table 5. Average Regional (Aqua-Terra) Difference of AOT at 550 nm for the Period of June 2002 to December 2003

Label	Name	$Avg^{A\text{-}T}AOT550diff$
	Land	
1	northwest America	0.035
2	central United States	0.018
3	eastern United States	0.036
4	Brazil	0.016
5	west Africa	−0.012
6	South Africa	0.020
7	western Europe	0.007
8	Middle East	0.016
9	India	0.016
10	Russia	0.063
11	China	0.003
12	Australia	0.010
	Ocean	
A	central Pacific	−0.005
B	Mid-Atlantic	−0.004
C	South Atlantic	−0.004
D	Mediterranean Sea	0.005
E	northern India	−0.004
F	Asian Pacific	0.001

points for every region appear to be almost symmetrically distributed about the zero line for both land and ocean. The amplitude of the day-to-day variation of $D^{A\text{-}T}\tau_{a550}$ in each region (i.e., the vertical point spread) is proportional to that of the corresponding τ_{a550} at any given time period. However, based on $Avg^{A\text{-}T}\tau_{a550}$, there is a small net morning-to-afternoon increase over land regions, except over west Africa, though the margin is very small ($-0.012 < Avg^{A\text{-}T}\tau_{a550} < 0.020$). The over-ocean regions show almost equal likelihood of increasing or decreasing with a very tiny margin ($-0.005 < Avg^{A\text{-}T}\tau_{a550} < 0.005$).

4.3. Terra and Aqua MODIS Synergism at Local Scale

[38] Terra and Aqua MODIS data can be combined in a convenient manner to monitor the local aerosol dynamics in any given location. Figure 10 shows the local (50 × 50 km) daily mean aerosol optical thickness (AOT) at three wavelengths (470, 550, and 660 nm) from Terra- and Aqua-MODIS over two sites: one in the eastern United States (GSFC) and the other in the Arabian Sea. The data, covering the period of June/July 2002, demonstrate the synergism between the twin sensors, whereby aerosol properties are retrieved from one of the MODIS sensors even when conditions do not allow retrieval from the other.

[39] Since GSFC is also an AERONET site, time series curves of AERONET τ_{a440} and τ_{a670} nm are superimposed on the top panel of Figure 10, which shows that on 7 July, when the smoke from the huge Quebec fire reached GSFC, there was no retrieval from Terra-MODIS, perhaps because of cloud cover, but Aqua-MODIS measures the dramatic increase in AOT. *Taubman et al.* [2004] shows a Terra-MODIS image of 7 July, with the dense smoke outflow from the Quebec fire reaching GSFC. Although AERONET does not provide level 1.5 or 2.0 AOT over GSFC on 7 July because their automatic cloud filter mistook the dense smoke for clouds, it was noted that "the τ_{a500} was estimated as ∼7 (highest ever recorded in AERONET monitoring) from the spectra in the longer wavelengths ($\tau_{a870} \sim 3$)" [*Eck et al.*, 2003, paragraph [5]]. *Colarco et al.* [2004] presented a detailed study of the dynamics of smoke transport from that remarkable Quebec fire event, as well as the effects of the smoke on the local and regional air quality; using satellite, airborne, and ground-based measurements as well as model and trajectory analysis techniques. In particular, *Colarco et al.* [2004] specifically point out the dense smoke outflow from the Quebec fire to GSFC on a 7 July visible image from the SeaWiFS sensor, while the TOMS sensor aerosol retrieval for that date also shows the AOT at 380 nm to be 5 or higher over GSFC.

[40] The bottom panel of Figure 10, representing a remote site over the Arabian Sea, shows where, by coincidence, data points or peaks from Terra and Aqua-MODIS alternate with one another. This provides for continuity in data, which could have been missed if only one instrument was involved. In both cases, there is beautiful agreement on dates having retrieval from both instruments.

5. Conclusions

[41] The spectral aerosol optical thickness $\tau_{a\lambda}$ data, produced from Terra-MODIS and Aqua-MODIS from the beginning (2000 and 2002, respectively) up till the end of 2003, have been comprehensively and comparatively evaluated using AERONET data. The data sets evaluated were versions 3 and 4 from Terra-MODIS (T003 and T004) and version 3 from Aqua-MODIS (A003), which was retrieved with almost the same algorithm version as T004. Global assessment of τ_{a550} from T003, T004, and A003, based on quality-assured (level 2.0) AERONET data, showed that about 67.5%, 55.0%, and 55.5% respectively, fall within the predefined uncertainty range of $\pm(0.05 + 0.2\ \tau_{a\lambda})$ over land, while about 63.3%, 59.4%, and 62.2%, respectively, fall within the more stringent over-ocean predefined range of $\pm(0.03 + 0.05\ \tau_{a\lambda})$. For each of the data versions (T003, T004, and A003), the success rate appears to increase with wavelength at least for the evaluated 470 nm to 870 nm wavelength range. Furthermore, as the percentages above show, T003 is slightly more accurate than the later versions (T004 and A003) because these latter versions included retrieval over less than ideal situations such as over brighter surfaces on land. Over land, there is high likelihood of overestimation at low aerosol loading ($\tau_{a550} < 0.20$), with about 55–65% of MODIS $\tau_{a\lambda}$ retrievals falling within the predefined uncertainty bounds. The accuracy improves at moderate loading ($0.20 < \tau_{a550} < 0.70$), with 70% or more of the retrievals at this range falling within the predefined uncertainty envelope. At high aerosol loading ($\tau_{a550} > 0.70$) corresponding to less than 2% of the total retrievals, the accuracy fluctuates erratically. Over ocean, MODIS accu-

Figure 9b. Eastern Hemisphere time series of regional daily average Terra-MODIS AOT at 550 nm (lower points, left scale) coplotted with the corresponding (Aqua-Terra) τ_{a550} differences (upper points, right scale). The regional averages were derived directly from MODIS level 2 (10-km resolution) aerosol data from Terra and Aqua before the (Aqua-Terra) τ_{a550} daily differences $D^{A\text{-}T}\tau_{a550}$ were calculated.

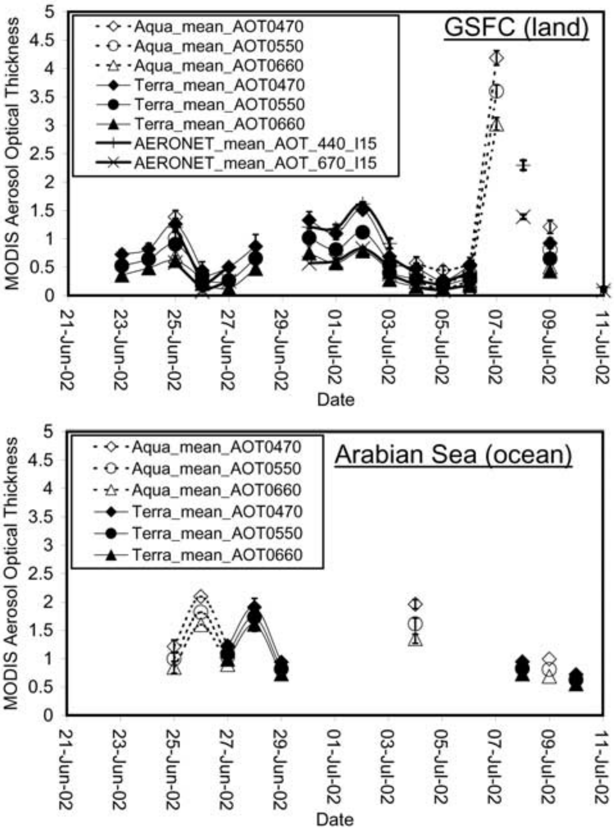

Figure 10. Local (50 × 50-km) daily mean Terra- and Aqua-MODIS aerosol optical thickness (AOT) at three wavelengths (470, 550, and 660 nm) over two sites (one in the eastern United States (GSFC) and the other in the Arabian Sea) in June/July 2002. Terra data are represented by thin solid lines and filled symbols, while Aqua data are represented by dotted lines and open symbols. AERONET mean AOT at 440 and 670 nm wavelengths (averaged within ±30 min of Terra or Aqua overpass) are superimposed on the GSFC panel (thick solid curves), since this is also an AERONET site, to demonstrate that MODIS (on Terra and Aqua) observed the same pattern of time series as the AERONET ground-based measurements. See color version of this figure at back of this issue.

racy is high at low aerosol loading, with over 80% of the retrievals in the range of $\tau_{a550} < 0.05$ falling within the uncertainty envelop. The over-ocean accuracy decreases as the aerosol loading increases. Although the global land and ocean percentages above seem comparable because of the more stringent tolerance over ocean, the respective correlation coefficients and regression slopes and intercepts show that the MODIS over-ocean retrievals are more accurate than over-land products. The main problems identified as influencing the over-land retrieval accuracy relate mainly to background land surface uncertainty due to surface variability, surface brightness, swamps, snow (especially at the melting stage). Other possible influences include scan angle dependence and neglecting to include polarization in the radiative transfer treatment. By contrast, the ocean retrieval, in addition to enjoying the benefit of a smoother dark (ocean) surface, which is favorable to aerosol retrieval (except over sun glint regions), also benefits from richer information content of the six wavelengths used directly for retrieval (as opposed to only two over land). Overall, the difference in performance between Terra and Aqua is not very significant.

[42] Evaluation of MODIS $\tau_{a\lambda}$ was also conducted at the regional level, to enable the perception of trends of regional performance over time, for easy quantitative application to studies dealing with aerosol distribution and climate forcing. For this aspect of the study, MODIS-AERONET (or M-A) τ_{a550} differences from collocated data were used, such that negative, near-zero, and positive differences would respectively signify underestimation, accurate estimation, and overestimation in the MODIS aerosol retrieval. There were significant regional differences in MODIS quality with respect to AERONET. For the 12 land and 6 ocean regions investigated, those with the most accurate retrievals (with overall average τ_{a550} differences of ±0.05 or less, with maybe one or two outliers) are: Russia and Brazil (over land), and the Mediterranean, Mid-Atlantic, north Indian and central Pacific Oceans (over ocean). The regions with tendency toward underestimation are west Africa and southern Africa (over land), and southern Atlantic and Asian Pacific (over ocean). This could be because of inaccurate model assumptions in the parameterization of aerosol spectral properties (e.g., assuming lower absorption than is truly the case with the predominantly highly absorbing southern African savanna smoke [*Ichoku et al.*, 2003], which was rectified early in the algorithm for T004 and A003). Regions with tendency toward overestimation are all over land and include: northwest America, central United States, eastern United States, western Europe, and India (with an overall average overestimation of the order of 0.05), and China, Middle East, and Australia (with an overall average overestimation of the order of 0.15).

[43] MODIS aerosol spectral optical thickness $\tau_{a\lambda}$ from Terra and Aqua are appreciably accurate over ocean, but have a slightly lower quality over land. However, the data can be used for various kinds of global, regional, and local studies with acceptable accuracy. Analysis of MODIS $\tau_{a\lambda}$ subdivided into three size ranges based on different AERONET Ångstrom exponent ranges ($\alpha < 0.7$, $0.7 < \alpha < 1.8$, and $\alpha > 1.8$, respectively representing large, midrange, and small size modes), shows that the $\tau_{a\lambda}$ values are more accurate over ocean than over land. Time series of the group monthly averages of data acquired over AERONET sites, both from Terra-MODIS and AERONET, show a net steady increase in the average loading of the large size mode ($\alpha < 0.7$) from 2000 to 2003, especially over ocean. MODIS regional monthly average τ_{a550} time series (based on full spatial sampling) show large variations in seasonal cycles between regions, but do not show a net increase of aerosol loading even over dust-dominated regions. There is great resemblance in the cyclic amplitude and phase between regions with common aerosol type, source, or distribution characteristics. Analysis of the regional daily mean τ_{a550} differences between Terra and Aqua for the various study regions show that, although there are daily differences between the morning and afternoon observations from the twin sensors in most regions, the magnitudes of which vary from region to region, none of the regions shows any consistent morning-to-afternoon increase or decrease in

aerosol loading. Combined plots of the Terra-MODIS and Aqua-MODIS $\tau_{a\lambda}$ at the local scale for an over-land urban and an over-ocean dust environments, both of which contained some smoke, show that Terra and Aqua observations can provide for data continuity at different temporal scales.

[44] Finally, the evaluation done in this study has been extensive, employing an unprecedented number of collocated MODIS/AERONET data point pairs: over 23,000 for Terra and over 10,000 for Aqua. Although MODIS $\tau_{a\lambda}$ accuracies do not reach AERONET accuracy levels (of 0.02), especially over land, given that MODIS is the first sensor used for operational aerosol retrieval at moderate scale both over land and ocean, and considering the numerous problems posed to aerosol retrieval by the surface background, especially over land, and the potential sampling mismatch in comparing averages from MODIS spatially variable data space and AERONET temporally variable data space, the overall performance of the Terra and Aqua twin MODIS sensors in aerosol retrieval is excellent. Nevertheless, the MODIS aerosol team continues to evaluate and understand the sources of uncertainty and continues to develop and implement strategies aimed at systematically eliminating as much uncertainties as possible in order to generate top quality products for all types of applications.

[45] **Acknowledgments.** This study was conducted as part of the MODIS aerosol retrieval and validation project, supported under the NASA Earth Observing System (EOS) program under the direction of Michael King. We would like to thank the various MODIS atmosphere software development and support teams for the production and distribution of the MODIS data, particularly the aerosol group led by Yoram Kaufman, who together with Didier Tanré formulated the MODIS aerosol algorithms. We are also very grateful to Yoram Kaufman for very helpful ideas and comments on this paper. We thank the AERONET PIs and team members for collecting, processing, and making available ground-based aerosol observations around the world. Special thanks go to Brent Holben (AERONET PI) for authorizing the use of the AERONET data and to Ilya Slutsker and David Giles for maintaining the AERONET data system and Web site and for compiling the data needed for MODIS validation. Indeed, the AERONET project has been very instrumental to the success of the validation of MODIS aerosol products, and much credit is due to those who conceived the idea of AERONET.

References

Christopher, S. A., and J. Zhang (2002), Shortwave aerosol radiative forcing from MODIS and CERES observations over the oceans, *Geophys. Res. Lett.*, *29*(18), 1859, doi:10.1029/2002GL014803.

Chu, D. A., Y. J. Kaufman, C. Ichoku, L. A. Remer, D. Tanré, and B. N. Holben (2002), Validation of MODIS aerosol optical depth retrieval over land, *Geophys. Res. Lett.*, *29*(12), 8007, doi:10.1029/2001GL013205.

Chu, D. A., Y. J. Kaufman, G. Zibordi, J. D. Chern, J. Mao, C. Li, and B. N. Holben (2003), Global monitoring of air pollution over land from the Earth Observing System-Terra Moderate Resolution Imaging Spectroradiometer (MODIS), *J. Geophys. Res.*, *108*(D21), 4661, doi:10.1029/2002JD003179.

Colarco, P. R., M. R. Schoeberl, B. G. Doddridge, L. T. Marufu, O. Torres, and E. J. Welton (2004), Transport of smoke from Canadian forest fires to the surface near Washington, D.C., Injection height, entrainment, and optical properties, *J. Geophys. Res.*, *109*, D06203, doi:10.1029/2003JD004248.

Dubovik, O., B. N. Holben, T. F. Eck, A. Smirnov, Y. J. Kaufman, M. D. King, D. Tanré, and I. Slutsker (2002), Variability of absorption and optical properties of key aerosol types observed in worldwide locations, *J. Atmos. Sci.*, *59*, 590–608.

Eck, T. F., B. N. Holben, J. S. Reid, O. Dubovik, A. Smirnov, N. T. O'Neill, I. Slutsker, and S. Kinne (1999), Wavelength dependence of the optical depth of biomass burning, urban, and desert dust aerosols, *J. Geophys. Res.*, *104*, 31,333–31,349.

Eck, T. F., B. N. Holben, J. S. Reid, N. T. O'Neill, J. S. Schafer, O. Dubovik, A. Smirnov, M. A. Yamasoe, and P. Artaxo (2003), High aerosol optical depth biomass burning events: A comparison of optical properties for different source regions, *Geophys. Res. Lett.*, *30*(20), 2035, doi:10.1029/2003GL017861.

Gao, B., Y. J. Kaufman, D. Tanre, and R. Li (2002), Distinguishing tropospheric aerosols from thin cirrus clouds for improved aerosol retrievals using the ratio of 1.38-μm and 1.24-μm channels, *Geophys. Res. Lett.*, *29*(18), 1890, doi:10.1029/2002GL015475.

Holben, B. N., et al. (1998), AERONET—A federated instrument network and data archive for aerosol characterization, *Remote Sens. Environ.*, *66*, 1–16.

Holben, B. N., et al. (2001), An emerging ground-based aerosol climatology: Aerosol optical depth from AERONET, *J. Geophys. Res.*, *106*, 12,067–12,097.

Ichoku, C., D. A. Chu, S. Mattoo, Y. J. Kaufman, L. A. Remer, D. Tanré, I. Slutsker, and B. N. Holben (2002), A spatio-temporal approach for global validation and analysis of MODIS aerosol products, *Geophys. Res. Lett.*, *29*(12), 8006, doi:10.1029/2001GL013206.

Ichoku, C., L. A. Remer, Y. J. Kaufman, R. Levy, D. A. Chu, D. Tanré, and B. N. Holben (2003), MODIS observation of aerosols and estimation of aerosol radiative forcing over southern Africa during SAFARI 2000, *J. Geophys. Res.*, *108*(D13), 8499, doi:10.1029/2002JD002366.

Ichoku, C., Y. J. Kaufman, L. A. Remer, and R. Levy (2004), Global aerosol remote sensing from MODIS, *Adv. Space Res.*, *34*, 820–827.

Kaufman, Y. J., D. Tanré, L. A. Remer, E. F. Vermote, A. Chu, and B. N. Holben (1997), Operational remote sensing of tropospheric aerosol over land from EOS moderate resolution imaging spectroradiometer, *J. Geophys. Res.*, *102*, 17,051–17,067.

Kaufman, Y. J., B. N. Holben, D. Tanré, I. Slutsker, A. Smirnov, and T. F. Eck (2000), Will aerosol measurements from Terra and Aqua polar orbiting satellites represent the daily aerosol abundance and properties, *Geophys. Res. Lett.*, *27*, 3861–3864.

Kaufman, Y. J., D. Tanré, and O. Boucher (2002), A satellite view of aerosols in the climate system, *Nature*, *419*, 215–223.

Koren, I., Y. J. Kaufman, L. A. Remer, and J. V. Martins (2004), Measurement of the effect of Amazon smoke on inhibition of cloud formation, *Science*, *303*, 1342–1345.

Levy, R. C., L. A. Remer, D. Tanré, Y. J. Kaufman, C. Ichoku, B. N. Holben, J. M. Livingston, P. B. Russell, and H. Maring (2003), Evaluation of the Moderate-Resolution Imaging Spectroradiometer (MODIS) retrievals of dust aerosol over the ocean during PRIDE, *J. Geophys. Res.*, *108*(D19), 8594, doi:10.1029/2002JD002460.

Levy, R. C., L. A. Remer, and Y. J. Kaufman (2004), Effects of neglecting polarization on the MODIS aerosol retrieval over land, *IEEE Trans. Geosci. Remote Sens.*, *42*(11), 2576–2583.

Lyapustin, A. I., and Y. J. Kaufman (2001), Role of adjacency effect in the remote sensing of aerosol, *J. Geophys. Res.*, *106*, 11,909–11,916.

Martins, J. V., D. Tanré, L. Remer, Y. Kaufman, S. Mattoo, and R. Levy (2002), MODIS Cloud screening for remote sensing of aerosols over oceans using spatial variability, *Geophys. Res. Lett.*, *29*(12), 8009, doi:10.1029/2001GL013252.

Remer, L. A., et al. (2002), Validation of MODIS aerosol retrieval over ocean, *Geophys. Res. Lett.*, *29*(12), 8008, doi:10.1029/2001GL013204.

Remer, L. A., et al. (2005), The MODIS aerosol algorithm, products and validation, *J. Atmos. Sci.*, in press.

Smirnov, A., B. N. Holben, T. F. Eck, O. Dubovik, and I. Slutsker (2000), Cloud screening and quality control algorithms for the AERONET data base, *Remote Sens. Environ.*, *73*, 337–349.

Smirnov, A., B. N. Holben, T. F. Eck, I. Slutsker, B. Chatenet, and R. T. Pinker (2002), Diurnal variability of aerosol optical depth observed at AERONET (Aerosol Robotic Network) sites, *Geophys. Res. Lett.*, *29*(23), 2115, doi:10.1029/2002GL016305.

Tanré, D., Y. J. Kaufman, M. Herman, and S. Mattoo (1997), Remote sensing of aerosol properties over oceans using the MODIS/EOS spectral radiances, *J. Geophys. Res.*, *102*, 16,971–16,988.

Taubman, B. F., L. T. Marufu, B. L. Vant-Hull, C. A. Piety, B. G. Doddridge, R. R. Dickerson, and Z. Li (2004), Smoke over haze: Aircraft observations of chemical and optical properties and the effects on heating rates and stability, *J. Geophys. Res.*, *109*, D02206, doi:10.1029/2003JD003898.

Yu, H., R. E. Dickinson, M. Chin, Y. J. Kaufman, B. N. Holben, I. V. Geogdzhayev, and M. I. Mishchenko (2003), Annual cycle of global distributions of aerosol optical depth from integration of MODIS retrievals and GOCART model simulations, *J. Geophys. Res.*, *108*(D3), 4128, doi:10.1029/2002JD002717.

T. F. Eck, NASA/GSFC (GEST), Code 923, Greenbelt, MD 20771, USA.

C. Ichoku and L. A. Remer, Laboratory for Atmospheres, NASA Goddard Space Flight Center, Code 913, Building 33, Room C323, Greenbelt, MD 20771, USA. (ichoku@climate.gsfc.nasa.gov)

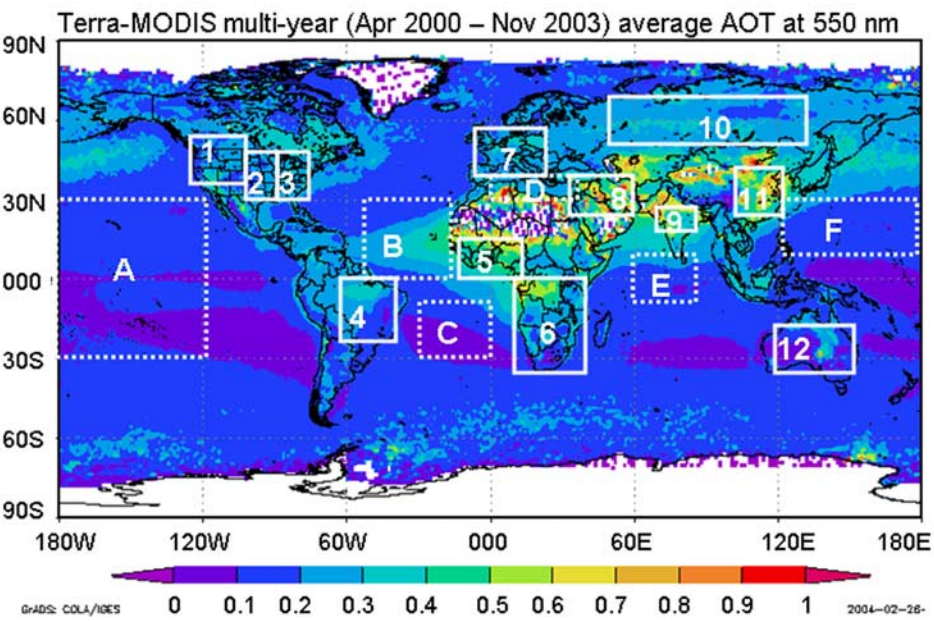

Figure 1. Multiyear (2000–2003) average aerosol optical thickness (AOT) at 550 nm wavelength from Terra-MODIS showing rectangular boundaries of various regions referenced in this study. Land regions are delimited by solid lines with numeric labels (1–12), while ocean regions are delimited by dotted lines with alphabetic labels (A–F). Since MODIS currently does not retrieve aerosols over highly bright surfaces such as Greenland, the Sahara, and the Antarctica, the purple patches (zero values) in those regions may be due to artifacts from the plotting software.

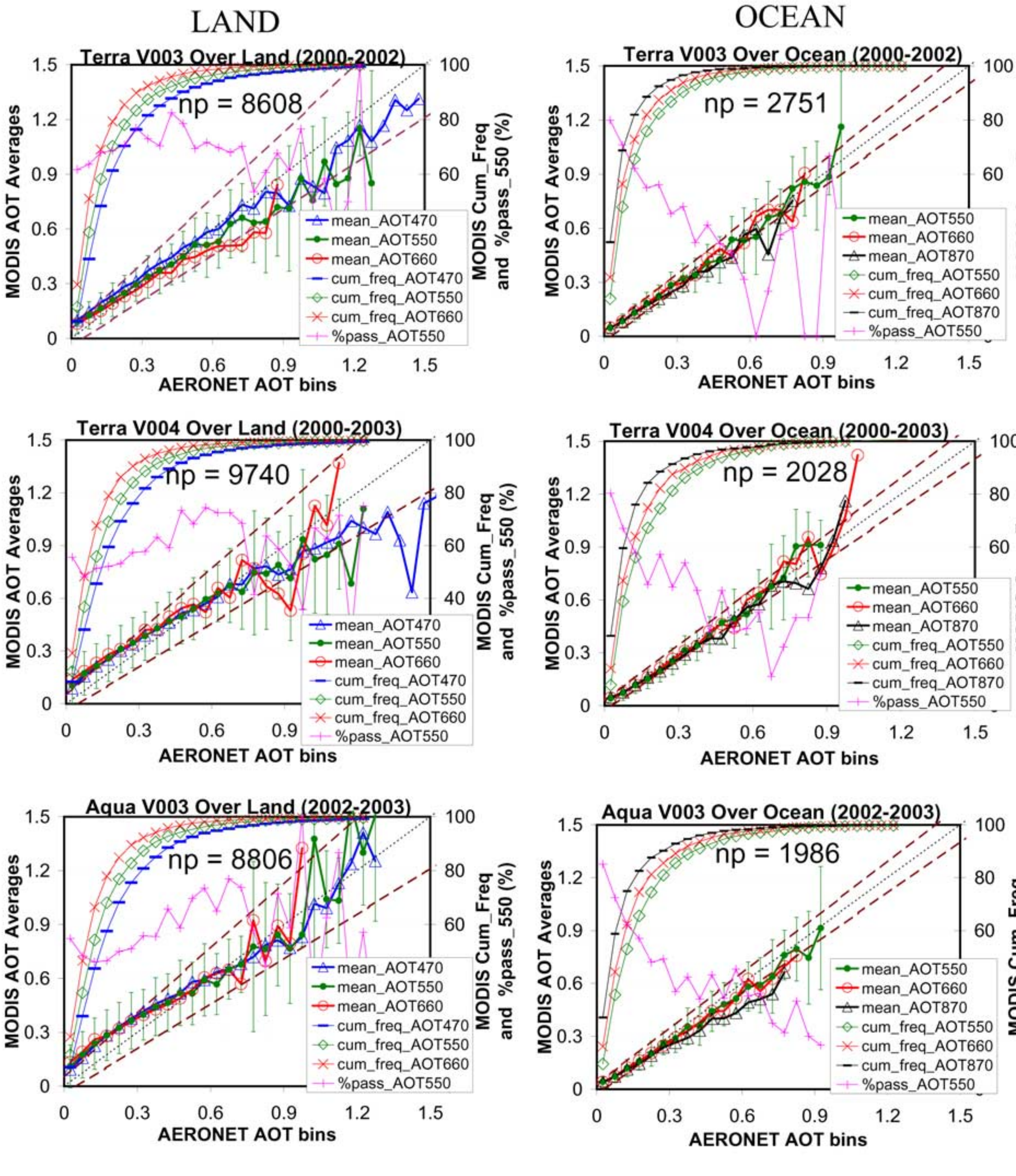

Figure 2. Modified scatterplots of MODIS global class average AOT (based on collocated AERONET AOT bins) against the AERONET AOT bin center values for T003, T004, and A003 over land (at 470, 550, 660 nm wavelengths) and ocean (at 550, 660, 870 nm wavelengths). The standard deviations of the AOT classes for MODIS are shown as error bars only for the 550 nm curves (to limit clutter). The dotted diagonal line is the 1-to-1 line, while the pair of near diagonal broken lines are the bounds of the uncertainty envelops. The total number of data points (*np*) used in each data group is shown on each panel, while the cumulative counts of data points in each class are plotted at all wavelengths represented. The percent proportion of MODIS AOT at 550 nm falling within the specified uncertainty bounds in each class are plotted (%pass_550).

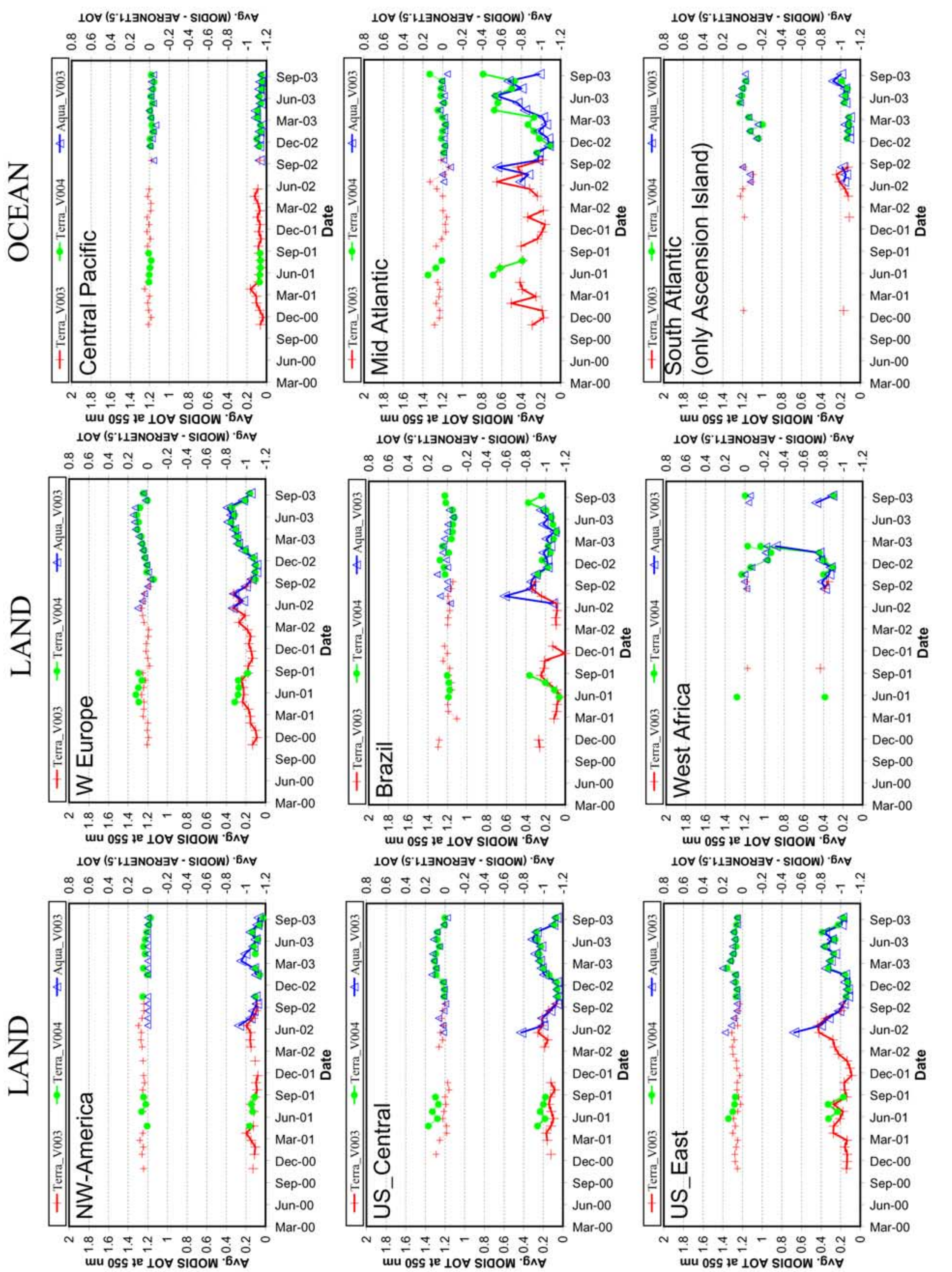

Figure 3a. Western Hemisphere time series of regional monthly mean AOT at 550 nm and corresponding (MODIS-AERONET) differences for the different MODIS aerosol data versions (T003, T004, and A003).

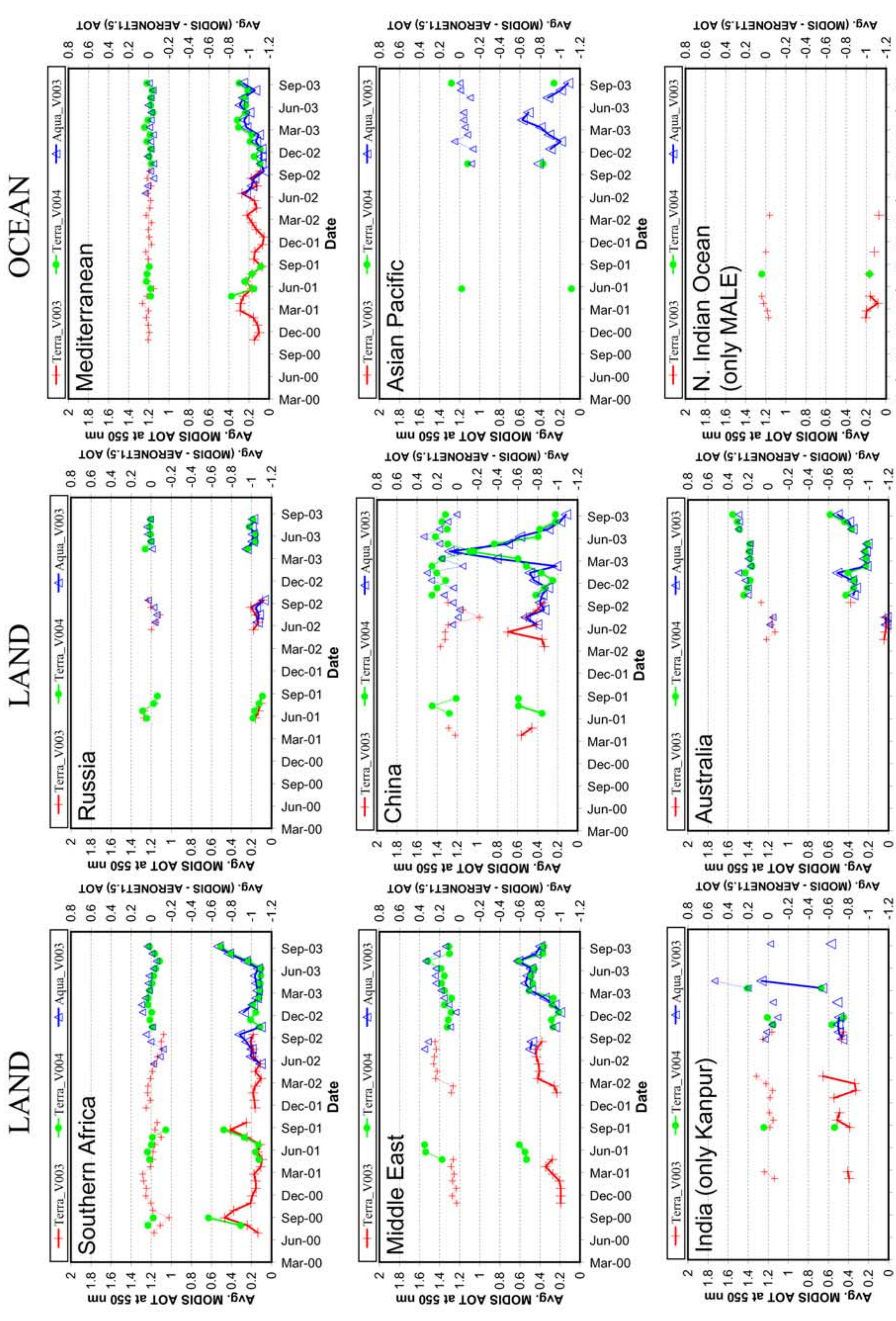

Figure 3b. Eastern Hemisphere time series of regional monthly mean AOT at 550 nm and corresponding (MODIS-AERONET) differences for the different MODIS aerosol data versions (T003, T004, and A003).

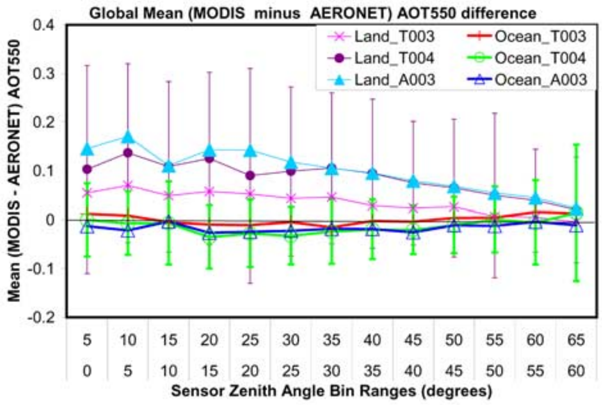

Figure 5. Plots of global mean (MODIS-AERONET) differences of AOT at 550 nm, grouped according to sensor zenith angle bins (5° intervals), for different Terra and Aqua MODIS data versions (T003, T004, and A003) over land (thin lines) and ocean (thick lines), plotted against their respective sensor zenith angle bins. Error bars (shown only for the land and ocean T004 to limit clutter) are the corresponding standard deviations.

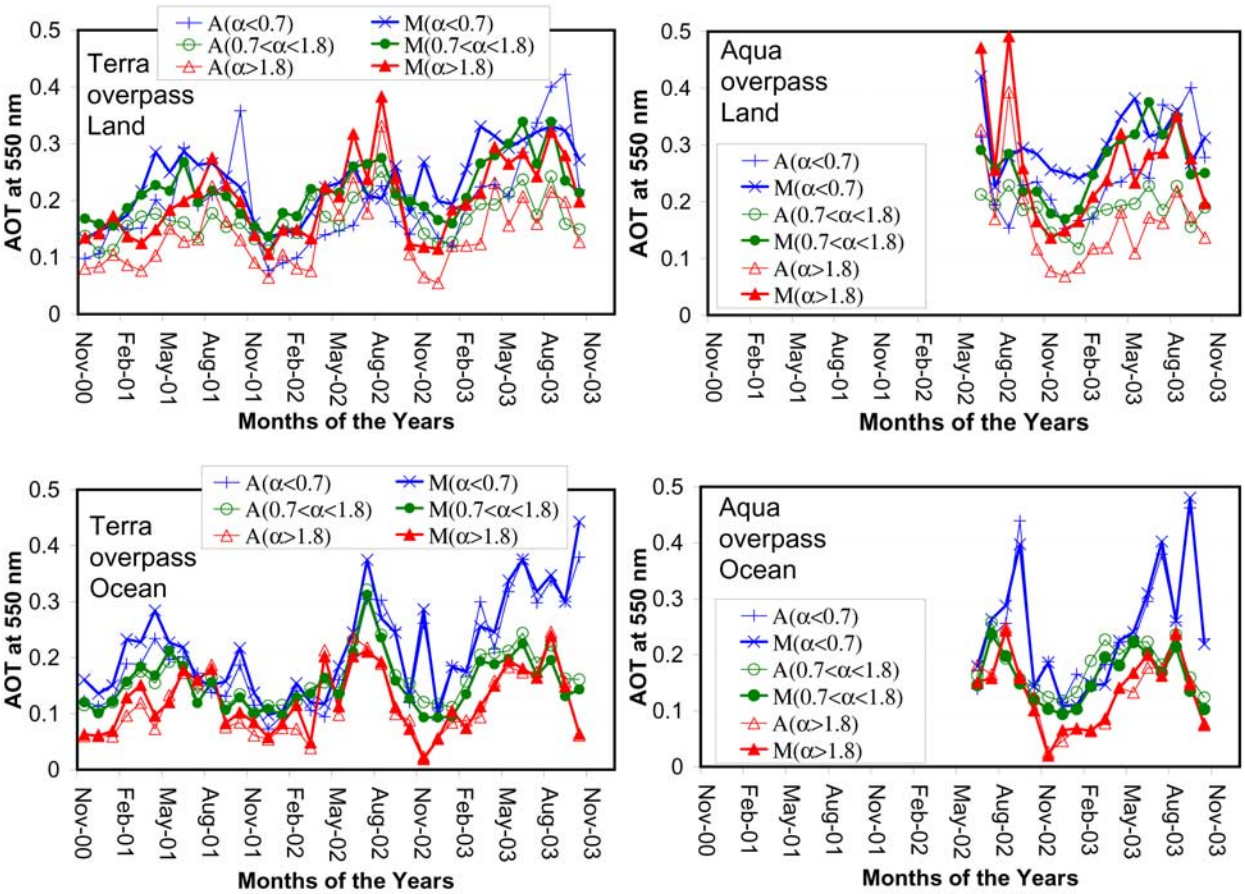

Figure 7. Monthly mean aerosol optical thickness (AOT) from MODIS and AERONET for the overpass times of Terra and Aqua over land and ocean. The averages were computed from local means (MODIS: 50 × 50 km; AERONET: ±30 min) over all AERONET stations grouped according to three ranges of AERONET Ångstrom exponent ($\alpha < 0.7$, $0.7 < \alpha < 1.8$, or $\alpha > 1.8$).

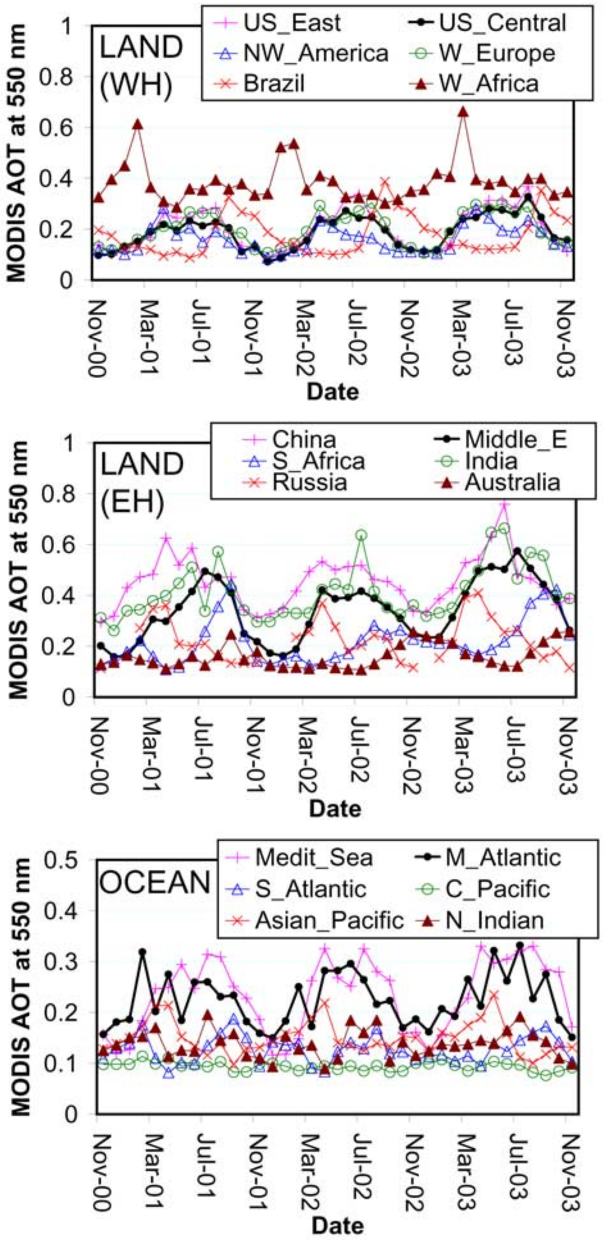

Figure 8. Time series of regional monthly average AOT at 550 nm, derived directly from MODIS level 2 (10-km resolution) daily aerosol products. The regions are grouped as (top) Western Hemisphere (WH) land, (middle) Eastern Hemisphere (EH) land, and (bottom) ocean. Note that the scale of the ocean panel is twice that of the land plots.

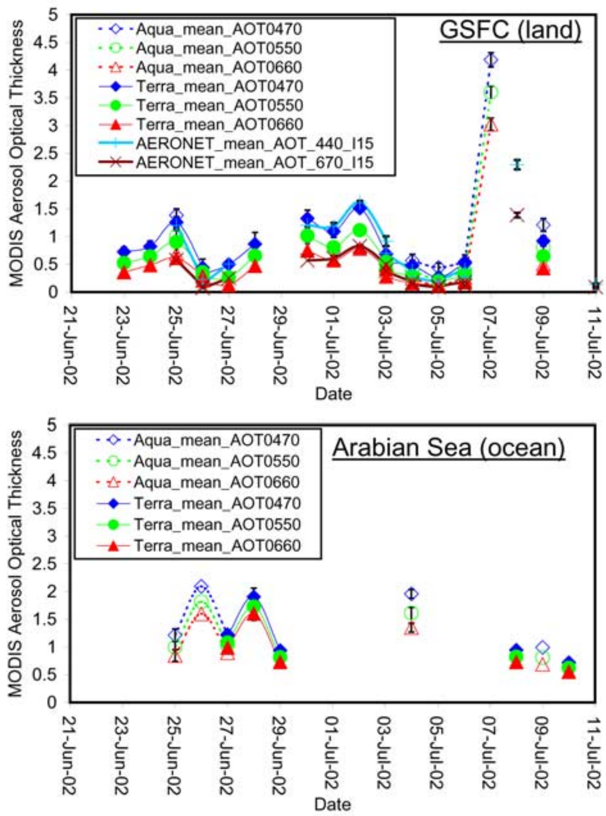

Figure 10. Local (50 × 50-km) daily mean Terra- and Aqua-MODIS aerosol optical thickness (AOT) at three wavelengths (470, 550, and 660 nm) over two sites (one in the eastern United States (GSFC) and the other in the Arabian Sea) in June/July 2002. Terra data are represented by thin solid lines and filled symbols, while Aqua data are represented by dotted lines and open symbols. AERONET mean AOT at 440 and 670 nm wavelengths (averaged within ±30 min of Terra or Aqua overpass) are superimposed on the GSFC panel (thick solid curves), since this is also an AERONET site, to demonstrate that MODIS (on Terra and Aqua) observed the same pattern of time series as the AERONET ground-based measurements.